Oil & Gas Science and Technology – Rev. IFP, Vol. 61 (2006), No. 1, pp. 95-119

Dossier

Development and Control of Combustion Systems
Évolutions et contrôle des systèmes de combustion

Nature of CAI Combustion and Air/Fuel Ratio Stratification Effects

B. Thirouard[1] and J. Cherel[1]

1 Institut français du pétrole, 1 et 4, avenue de Bois Préau, 92852 Rueil-Malmaison Cedex - France
e-mail: benoist.thirouard@ ifp.fr - jerome.cherel@ifp.fr

Résumé — Nature de la combustion CAI et impact de stratifications de richesse — La combustion CAI (Controlled Auto-Ignition) appliquée aux moteurs essence permet un fonctionnement en mélange pauvre avec de très faibles émissions d'oxyde d'azote. De ce fait, ce procédé de combustion présente un fort potentiel pour la réduction de consommation des motorisations essence. Les travaux décrits visent à approfondir la compréhension des phénomènes physiques et chimiques qui régissent l'auto-inflammation et les différentes étapes du déroulement de la combustion en fonctionnement CAI. En particulier, l'étude s'est intéressée à la phase d'apparition des précurseurs de l'auto-inflammation qui précède la phase de dégagement de chaleur et à l'analyse de la structure de zone de combustion. Ces travaux ont été réalisés sur moteur optique à l'aide de visualisation directe de la combustion et de fluorescence induite par laser pour la détection des intermédiaires de combustion OH et formaldéhyde. Il est apparu que le fort taux de dégagement de chaleur qui est caractéristique du fonctionnement CAI est dû à une combustion qui se déroule en volume, et qui localement présente un taux de réaction modéré. Le contrôle du taux de dégagement de chaleur ne peut par conséquent être maîtrisé que par une stratification du mélange visant à diminuer la quantité de gaz en combustion à un instant donné, ou par une dilution renforcée visant à diminuer le taux de réaction. De fait, l'influence de la qualité du mélange air/carburant/gaz résiduels sur l'auto-inflammation et le déroulement de la combustion a été étudiée. Pour cela, le mélange a été caractérisé à l'aide de technique de fluorescence induite laser sur traceur et le déroulement de la combustion a été observé à l'aide d'une caméra rapide intensifiée. Une analyse cycle à cycle de la répartition des sites d'auto-inflammation et du champ de richesse locale a montré que les premières zones de réaction apparaissaient préférentiellement dans les hétérogénéités du mélange les plus riches en carburant. De plus, il est apparu que le niveau de stratification de la charge obtenu par l'utilisation d'injection indirecte dissymétrique ne permet pas de modifier le déroulement de la combustion. Enfin, l'utilisation de l'injection directe a été testée et a montré qu'il était possible de contrôler le phasage de l'auto-inflammation par l'utilisation de stratégies d'injection appropriées simples ou multiples. La création d'une zone riche à délai réduit lors d'injection tardive et la pré-décomposition du carburant lors d'injection pendant la phase de recompression sont apparus être les principaux phénomènes responsables de l'impact de la stratégie d'injection sur le phasage de la combustion.

Abstract — Nature of CAI Combustion and Air/Fuel Ratio Stratification Effects — *The purpose of this study was to gain a better understanding of the fundamental aspects of the CAI combustion process in order to assess the possibilities of controlling CAI combustion through air/fuel mixture stratification. The experimental work was conducted on a single-cylinder gasoline engine equipped with optical accesses. Two engine configurations (NVO—Negative Valve Overlap—and EGRB—Exhaust Gas Re-Breathing) were tested.*

Investigation of the combustion process using optical diagnostics showed that CAI combustion is characterized by auto-ignition reactions triggering simultaneous combustion in large volumes of fresh gases. The high global heat release rate results from combustion reactions with moderate local chemical reaction rate occurring over a large volume of the burning gases.

From this analysis, it was concluded that controlling the heat release rate in CAI operation implies limiting the volume of the reaction zone by charge stratification, or decreasing the reaction rate by increasing the dilution. Consequently, a significant part of the work was focused on the investigation of the correlation between the fuel/air mixture quality and the CAI combustion process. It was found that low level of fuel stratification obtained with asymmetric port fuel injection does not significantly affect the combustion phasing even though it directly influences the location of the auto-ignition zones. Indeed, single cycle observations of the fuel distribution and the combustion process showed that the location of the first auto-ignition zones is strongly correlated with the position of the fuel rich areas.

Finally, direct fuel injection was found to provide a potential mean of controlling auto-ignition timing and to some extend the heat release rate. Combining multiple injections during the negative overlap period, the intake stroke and in the late compression stroke, the auto-ignition delay may be accurately adjusted to optimize the heat release phasing. It is believed that the control capability offered by multiple direct fuel injections can be used to extend the CAI operating range and further improve the fuel efficiency benefits.

INTRODUCTION

Combustion of a premixed-charge by compression ignition is a promising alternative combustion process as it allows part load operation with high dilution rate (air and/or residual gas dilution) while preserving engine stability. This combustion process attracted attention on account of its potential for achieving high efficiency and ultra-low NOx emissions [1-4]. When using commercial gasoline as fuel, auto-ignition of a premixed charge in a four-stroke engine can be achieved with high compression ratio, inlet air heating or residual gas trapping. CAI™ (Controlled Auto-Ignition) refers to auto-ignition combustion obtained with a high proportion of burned gases trapped in the fresh mixture. The mechanisms which promote auto-ignition probably involve both thermal and chemical effects of the recycled burned gases. While numerous studies showed that the heating effect is predominant [5, 6], a few ones emphasized the active role of chemical species like CO, H_2 and NO [7].

Most attempts to apply the CAI combustion process in passenger car engines have pointed out that two major issues are the limited load range over which this combustion process can be used and the difficulty of controlling the timing of auto-ignition [4]. Both issues are related since controlling the combustion phasing may help increasing the CAI combustion range toward both low and high load.

Many attempts to control the combustion phasing and duration have been reported. The most adequate way of controlling auto-ignition phasing in CAI configuration is to control the amount of burned gases recycled by an accurate valve timing and possibility valve lift management. Such CAI combustion control has been demonstrated in a single cylinder engine in Negative Valve Overlap [8] and Exhaust Gas Re-Breathing [9] configurations. The technique was also applied with success in multi-cylinder engine running in a Negative Valve Overlap CAI configuration [10]. Inlet air temperature management was proposed and applied for HCCI combustion control [11, 12]. One of the main drawbacks was found to be the time response of intake air control system. Moreover, because in CAI mode most of the heat required to promote auto-ignition is provided by the burned recycled gases, controlling the combustion phasing by thermal management of the intake air is not appropriate [13]. Closed-loop combustion phasing control was achieved with acceptable performance using variable compression ratio (VCR) and variable cylinder to cylinder lambda in a HCCI engine [14-16]. However, because VCR requires a significant sophistication of the engine design, alternative mean of the combustion control would be preferred. Eventually, in recent work [17, 18] the benefits of using direct injection for CAI combustion phasing control was demonstrated. Single or multiple injections in the NVO phase, the intake and compression strokes were used to promote and/or delay the onset of auto-ignition in order to improve the fuel consumption benefits and expand the CAI operating range.

The nature of the CAI combustion process is drastically different from typical spark-ignited flame front propagation. Even though a great deal of effort was put into assessing the structure of premixed-charge auto-ignition combustion, it is believed that CAI combustion is not a mature combustion process. The objectives of this study were first to provide a thorough understanding of the nature of the combustion process, and secondly to investigate mixture quality effect and evaluate the potential for combustion control by mixture management.

Accordingly, the first part of this study was dedicated to the investigation of the fundamental aspects of CAI

combustion nature. In particular, the work focused on the analysis of the mechanism responsible for the spatial extension of the combustion thorough the chamber. Concerning mixture quality effects on compression ignition combustion, most of the work reported in literature was done in HCCI combustion where the main role of recycled burned gases is not to promote auto-ignition but to slow down the heat release process. Consequently, mixture quality effect on both the auto-ignition process and the CAI combustion extension phase are not well understood. While in HCCI operation, most of the heat required for mixture auto-ignition is provided by the compression work, in CAI combustion, burned gases while being mixed to the air/fuel mixture, not only act as thermal capacity that may slow the combustion process but more importantly carries the heat required for the onset of auto-ignition. Thus, the distribution of residuals gases in the fresh mixture is believed to be a key parameter in the CAI combustion process and part of this work was focused on the study of air/fuel/burned gases mixture quality effects. Eventually, in order to gain some understanding on the effects of fuel distribution on the CAI combustion process and thus some insights on the auto-ignition control mechanisms offered by appropriate direct or port injection strategies, part of the work was dedicated to the investigation of fuel stratification and fuel/air mixture inhomogeneities effects on the timing and location of auto-ignition.

The approach chosen is this work was to use research tools such as optical engine and advanced diagnostics to provide data on the mixture, the auto-ignition process and the structure of the reaction zone.

1 EXPERIMENTAL SETUP

1.1 Engine

1.1.1 Main Characteristics

The study was conducted on a single-cylinder gasoline engine equipped with a 4-valves pentroof combustion chamber. The main engine characteristics are shown in Table 1. Taking advantage of the fully separated intake ports and the natural symmetric tumble motion of the pentroof chamber, stratification of the fresh gases could be generated by feeding the engine with different mixture in each ports [19].

TABLE 1

Engine characteristics

Type	Four-valve pentroof
Bore x Stroke (mm)	82 x 83.5
Displacement (cm^3)	441
Compression ratio	11.4
Fuel 1	SP 95 (Euro95)
Fuel 2 (for LIF)	PRF 65

The engine was equipped with three optical access: two quartz windows in the cylinder head and one in the piston crown allowing combustion chamber visualization with a 45° mirror located in the elongated piston (see *Fig. 1*).

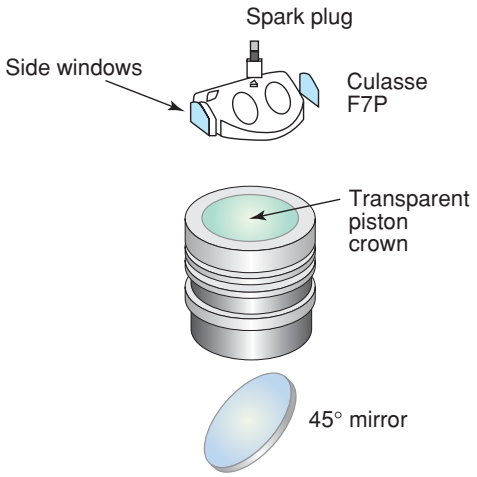

Figure 1

Engine optical access.

Two fuel injection systems were used:

– Port fuel injection with one injector in each intake port (injection pressure: 4 bar). Injector deactivation was used to allow asymmetric fueling and generate a stratification of the air/fuel ratio field.
– Direct injection with a Siemens DKDI (spray angle 60°) swirl injector located along the vertical axis in the center of the combustion chamber (injection pressure 70 bar).

1.1.2 Valves Actuation Strategies

To run the engine in CAI mode, a large quantity of residual gas is required to promote auto-ignition during the compression stroke. Two specific exhaust and intake valves timing strategies were used to significantly increase the amount of hot burned gas mixed in the fresh mixture (see *Figs 2 and 3*):

– Negative Valve Overlap (NVO): In this case, the early closing of the exhaust valves traps a large amount of residual gases in the combustion chamber. In parallel, a late intake valve opening is used to limit the back flow of burned gases into the intake ports (see *Fig. 2*). During the negative valve overlap, residual gases are compressed up to Top Dead Center (TDC) and a significant heat loss to the walls occurs.
– Exhaust Gas Re-Breathing (EGRB): In this configuration, the exhaust valve is first opened during the exhaust stroke and secondly re-opened during the intake stroke. During the second opening, burned gases that have been

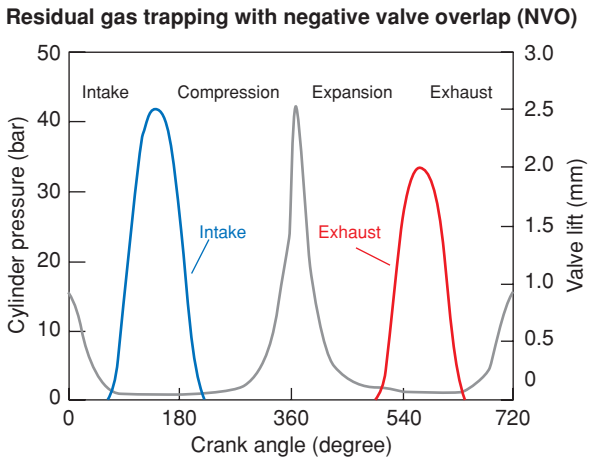

Figure 2

Valve actuation for the NVO residual gas trapping strategy.

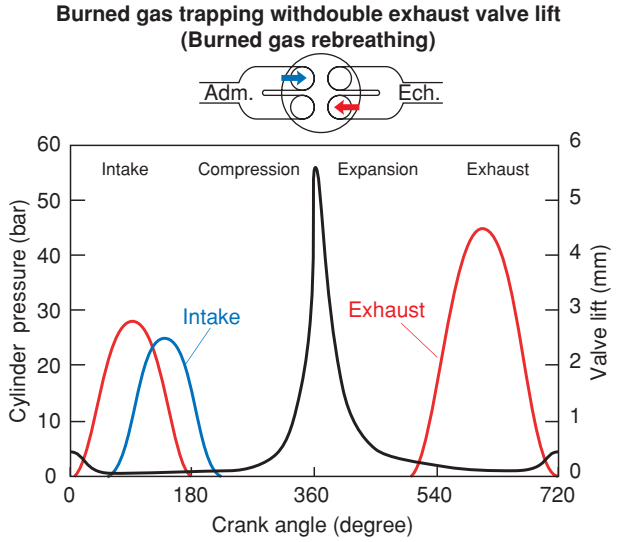

Figure 3

Valve actuation for burned gas re-breathing strategy.

previously expelled from the combustion chamber are re-admitted simultaneously with the fresh gases. In this operating mode, one intake and one exhaust valves located along the diagonal of the combustion chamber were deactivated.

The two valves actuation strategies define two CAI operation modes with different operating range. As a matter of fact, NVO is more appropriated for low to very low load operation while EGRB is more suitable for intermediate load. Consequently, these two strategies were studied on different operating points, which are defined in Table 1.

The residual gas rates obtained in tested running conditions were evaluated using a 0-D simulation code and found to be 51.6% in NVO configuration and 47.3% in EGRB configuration. The equivalence ratio of the mixture fed into the engine was monitored with a lambda probe in the exhaust pipe. Due to the high proportion of residual gas containing oxygen trapped in the combustion chamber, the equivalence ratio measured by the lambda probed differs significantly from the one of the combusting mixture when the fresh mixture is lean (see *Table 2*).

TABLE 2

Operating conditions tested in both NVO and EGRB configurations

Configuration	NVO	EGRB
Speed (rpm)	1200	1200
Vol. efficiency	0.30	0.38
Air flow rate (kg/h)	5.70	7.27
Equivalence ratio (Intake)	0.83	0.95
Equivalence ratio (Comb.)	0.69	0.91
Residual gas rate	51.6	47.3
IMEP (bar)	2.9	4.8

1.2 Direct Observation of the Combustion Chemiluminescence

1.2.1 High-Speed Combustion Imaging

The temporal and spatial development of the CAI combustion process was monitored by direct observation of the naturally emitted light. A 12-bit high speed intensified CCD camera (USS LaVision) and a 105 mm UV Nikkor lens were used to image the chemiluminescence emission from hot reacting gases. In lean HCCI operating conditions, Hulqvist *et al*. [20] showed that the chemiluminescence intensity is fairly proportional to the local reaction rate. A similar result was found in CAI combustion by comparing the average chemiluminescence intensity and the heat release rate computed from the cylinder pressure trace (see *Fig. 5*). As shown in Figure 4, because the direct observation of the combustion light is realized through the transparent piston crown the signal detected by the CCD camera is integrated along the vertical axis of the combustion chamber. Thus, intense light emission can be interpreted either as strong local reaction rate or as a reaction zone extended along the vertical axis of the chamber.

1.2.2 Auto-Ignition Sites Localization

Direct-observation images acquired at the beginning of the combustion process can be used to localize the first auto-ignition kernels. A sequence of post processing operations involving the following steps was applied to the chemiluminescence images in order to determine the contours and centers of the detected reaction zones:

– noise subtraction and noise reduction;
– image thresholding for identification of the reaction zones;
– reaction zone contour detection;

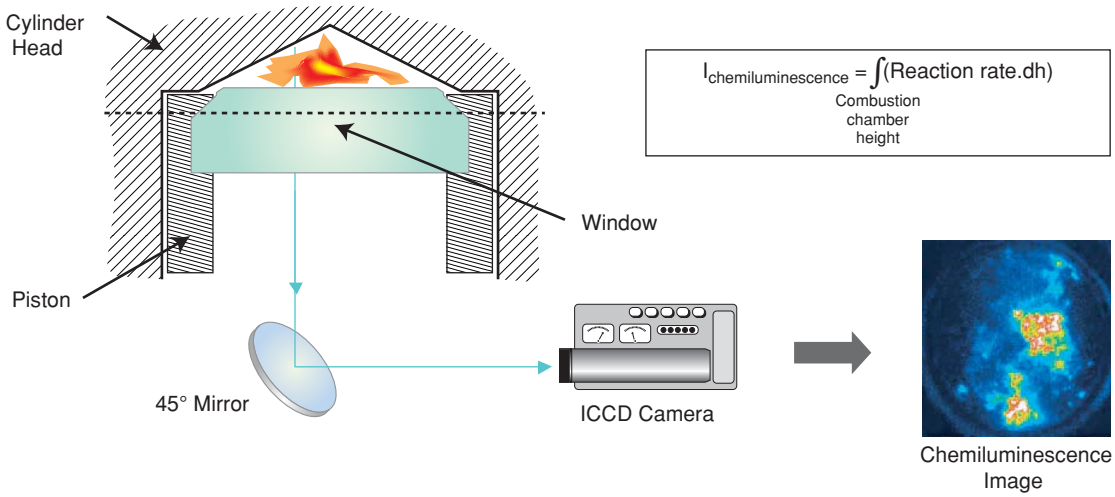

Figure 4

Schematic diagram of the experimental arrangement for direct observation of the combustion development.

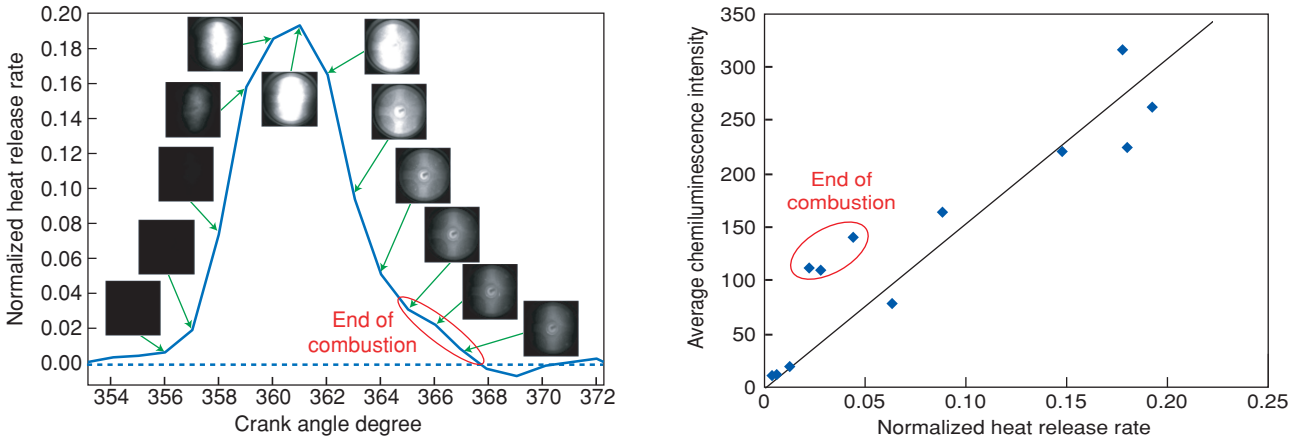

Figure 5

Comparison of the chemiluminescence intensity and the normalized heat release rate.

– computation of the intensity-weighted auto-ignition centers.

Using this post-processing procedure, large number of images could be automatically processed for statistical analysis.

1.3 LIF Imaging of the Fresh Mixture

1.3.1 Air/Fuel Ratio Distribution

Planar Laser Induced Fluorescence (LIF) was used to image the fuel distribution in the combustion chamber. Several studies including previous work conducted at *IFP* concluded that acetone was an appropriate fuel tracer in CAI running conditions [21]. In particular, it was found that acetone has a good resistance to thermal decomposition even in auto-igniting conditions characterized by high concentrations of hot residual gases. Moreover oxygen quenching of acetone fluorescence was observed to be very limited in the tested thermodynamic conditions. Therefore, acetone was chosen as tracer to characterize the fuel distribution in the combustion chamber. Acetone boiling temperature (56°C) is rather low compare to iso-octane and n-heptane, which are the two constituents of PRF65 fuel used for the LIF experiments. However, because the evaporation takes place in the intake ports, the different boiling characteristics of the fuel and tracer are not expected to affect significantly the fuel distribution imaging results. Excitation was realized with the fourth harmonic of a Nd-YAG laser (266 nm). A laser sheet formed with 90-mJ laser pulses was passed through the

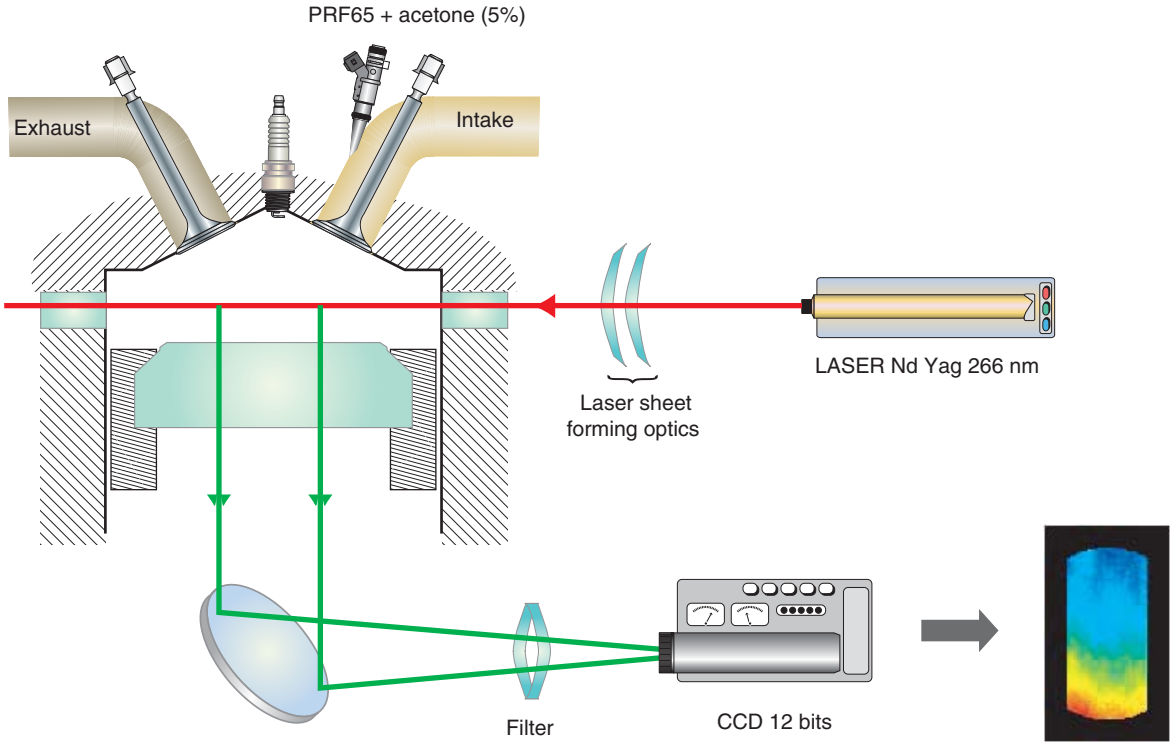

Figure 6

Schematic diagram of the experimental arrangement for LIF imaging of the fuel distribution.

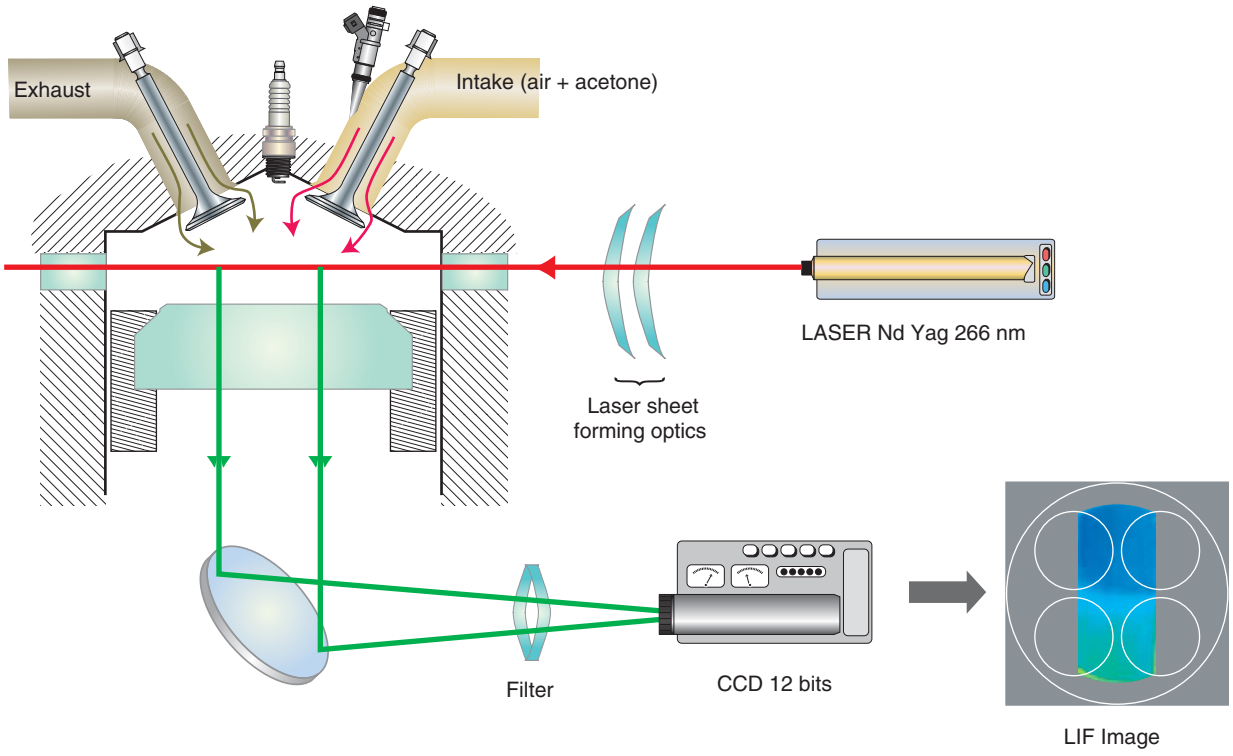

Figure 7

Schematic diagram of the experimental arrangement for LIF imaging of the air/burned gas mixture.

cylinder head side windows along the pentroof axis of the combustion chamber (see *Fig. 6*). LIF images were captured through the transparent piston crown with an intensified CCD camera (Princeton 12-bit Pentamax or 12-bit USS LaVision) and a 80-mm Nikkor lens. The non-UV lens was used to filter out laser reflections. The LIF images were post-processed to allow for the following corrections:

- noise subtraction;
- laser pulse to pulse energy variations (corrections were based on single pulse energy monitoring);
- laser sheet inhomogeneities (corrections were based on a 200-cycle averaged laser sheet image acquired in non-firing conditions with homogeneous intake air seeding).

Eventually, the fuel concentration field was calibrated using the hypothesis that the average signal intensity in the LIF image was equal to the average fuel concentration in the combustion chamber estimated from the lambda probe equivalence ratio measurement. The LIF signal calibration provided a quantitative information on the fuel concentration inhomogeneities ([fuel] = $mol._{carb}/(mol._{carb} + mol._{air} + mol._{residual\ gases}$). The computation of the local equivalence ratio from the fuel concentration requires an estimation of the oxygen concentration which is greatly affected by the local residual gas concentration. Consequently, in the present work the equivalence ratio could only be computed assuming a homogeneous residual gas distribution thorough the combustion chamber.

1.3.2 Residual Gas Distribution

A similar experimental setup to the one used for fuel distribution visualization was used to generate LIF images of the air/residual gas mixture. For the observation of residual gas distribution, acetone was used as a tracer of the fresh mixture. The acetone was atomized and mixed into the intake air using a Venturi-type diffuser located 2 meters upstream of the cylinder head. The LIF images obtained with this technique showed intense fluorescence signal in the region with low residual gas concentration and dark zones in areas of high burned gas content (see *Fig. 7*). A similar approach using biacethyl as tracer was used by Deschamps *et al.* [22] to visualize the residual gas distribution in a spark ignition engine. In this work, acetone was preferred to biacethyl for its good resistance to thermal decomposition. Depending on the thermodynamic conditions and excitation wavelength, fluorescence emission of acetone may exhibit a significant temperature dependence. In these experiments, employing excitation at 266 nm the sensitivity to temperature change is fair [23-26] and in any case implies a decay of the

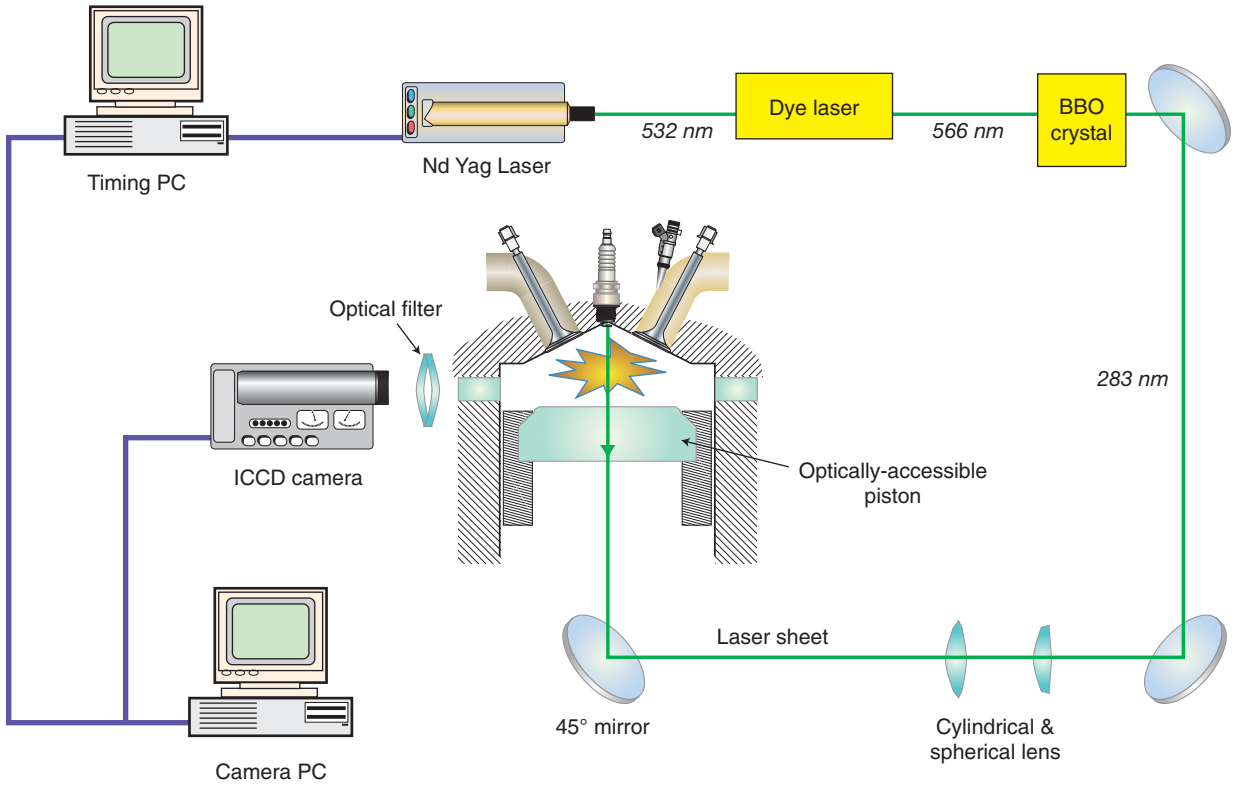

Figure 8

Experimental setup for LIF imaging of the OH radical distribution in a vertical plane.

fluorescence signal with increasing temperature [27]. Consequently, spatial fluctuations in the fluorescence signal may be attributed to composition and/or temperature variations in the gas mixture. In our application, the recycled burned gases being significantly hotter than the intake air, the inhomogeneities in the air/residual gas mixture are emphasized by the temperature dependence of the acetone LIF technique.

This technique also relies on the fact that fuel distribution inhomogeneities in the air/fuel mixture do not cause significant spatial fluctuations of the fluorescence signal. Based on the facts that:

– the molar proportion of fuel in the intake air is low (<2%);
– thanks to port fuel injection the air/fuel mixture is rather homogeneous, an estimation of the effect of fuel distribution heterogeneities on the LIF signal collected from acetone mixed in the intake air was found to be negligible.

Overall, this technique, which does not provide quantitative measurement of the local burned gas concentration, appeared to be appropriate for qualitative investigation of the air/residual gas mixture quality, both for cycle-averaged and single shot imaging.

1.4 LIF Imaging of Combustion Intermediate Species

1.4.1 OH Radical Distribution

OH imaging by laser-induced fluorescence was used to observe the structure of the combustion zone in CAI operation. Because OH radicals are produced during the combustion process and may be detected in the burned gases as long as temperature remains high enough, reaction zones and hot burned gases can be detected and observed with the 2D OH-LIF imaging technique [28-30].

The experimental setup employed for the in-cylinder LIF imaging of the OH radical distribution is shown in Figure 8. A 650 mJ pulse from a Nd:YAG laser at a wavelength of 532 nm and 10 Hz repetition rate was used to pump a tunable dye laser (Continuum ND6000) which contained a solution of Rhodamine 590. A BBO crystal allowed frequency doubling of the output pump beam from the dye laser permitting excitation between 280 and 284 nm. The experiments reported in the present study were conducted at an excitation wavelength of 283.93 nm. The laser energy within the combustion chamber was about 15 mJ per pulse. The fluorescence signal was captured by a 16-bit intensified CCD camera equipped a 45-mm UV lens. In order to isolate the LIF fluorescence signal (at approximatly 310 nm) from interference caused predominantly by laser elastic scattering and PAH fluorecence, a combination of optical filters was used.

1.4.2 Formaldehyde (CH_2O) Distribution

Formaldehyde is known to be an intermediate species which is present during the beginning of the auto-ignition process of hydrocarbons [31-33]. In order to detect the appearance of CH_2O in the combustion chamber, the third harmonic of a Nd:YAG laser was used to provide excitation at 355 nm. Excitation at 355 nm does present a number of drawbacks. Firstly, this particular wavelength only allows excitation of weak transitions in the CH_2O molecule [32] and unlike selective wavelength excitation [31], does not allow the discrimination of the formaldehyde signal against non-resonant signal contributions, notably from the fluorescence of PAH [34]. The experimental setup used for CH_2O observation was largely similar to that described for OH LIF imaging. The LIF 355 signal was isolated using a band-pass filter (400-480 nm). Additionally, to verify that the collected LIF 355 signal was due to CH20 fluorescence, an emission spectrum was measured (see *Fig. 9*) and compared to similar measurements reported by Böckle [31].

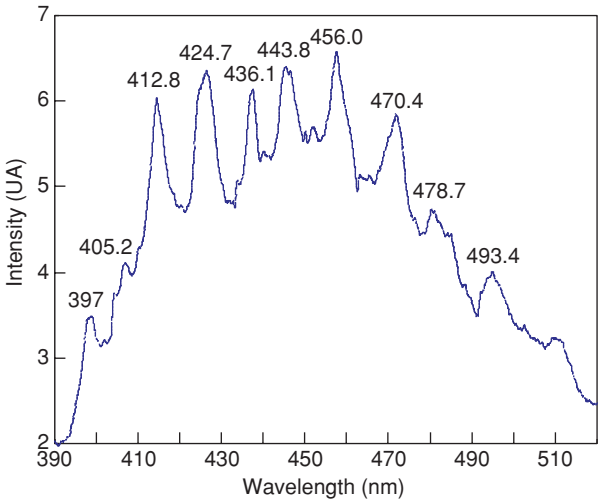

Figure 9

Fluorescence emission spectrum recorded in CAI operation at 355°CA.

1.5 Fuel for LIF Imaging

LIF imaging requires a non-fluorescent fuel to avoid fluorescence spectral interference. Because of its strong resistance to auto-ignition in CAI conditions, iso-octane which is commonly substituted to commercial gasoline for spark ignition engine studies could not be used in this work. A series of Primary Reference Fuel (PRF) were tested in the NVO configuration and compared with commercial gasoline Euro 95. The comparison was done using the cylinder pressure trace average over 200 cycles (see *Fig. 10*). The objective was to identify a fuel which displays similar combustion phasing and heat release rate on the tested operating point in the NVO CAI configuration. As shown in Figure 10, PRF65 appeared to be best suited. It exhibits a slightly longer auto-ignition delay and faster heat release rate than Euro95. Due to significantly higher heat release rate

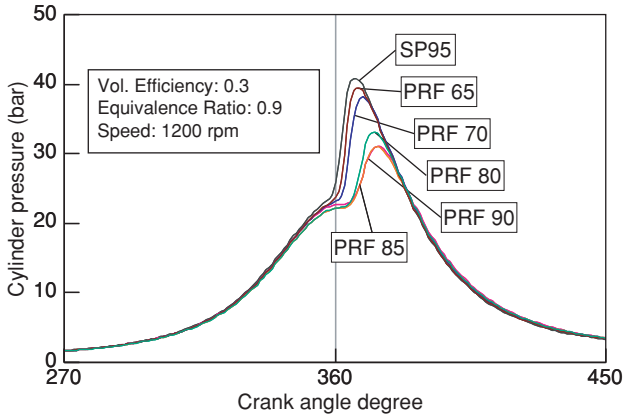

Figure 10

Comparison of pressure traces obtained with Primary Reference Fuels and Euro 95 commercial gasoline.

PRF60 was not considered. These results confirmed that octane number is not an appropriate indicator of the fuel auto-ignition ability in CAI operation [35].

2 COMBUSTION PROCESS ANALYSIS

Direct observation of the combustion light emission provides information on the auto-ignition phase and the main combustion process. In CAI combustion mode, multiple auto-ignition sites may appear simultaneously in various regions of the combustion chamber. Moreover the location of the initial reaction zones may vary greatly from cycle to cycle [32]. Therefore, a high-speed imaging system able to capture the complete combustion phase within a single cycle is necessary to properly investigate the combustion process. In this work, a Ultra Speed Star LaVision camera and a UV lens were used to observe the evolution of the chemiluminescence emission during the combustion phase. The camera is intensified, allowing for direct observation of the weak blue chemiluminescence emission and is able to capture 16 images at equivalent frequencies of up to 1 MHz.

2.1 Combustion in NVO Configuration

The 16-image sequence of Figure 11 shows a example of temporal evolution of the combustion phase observed in CAI

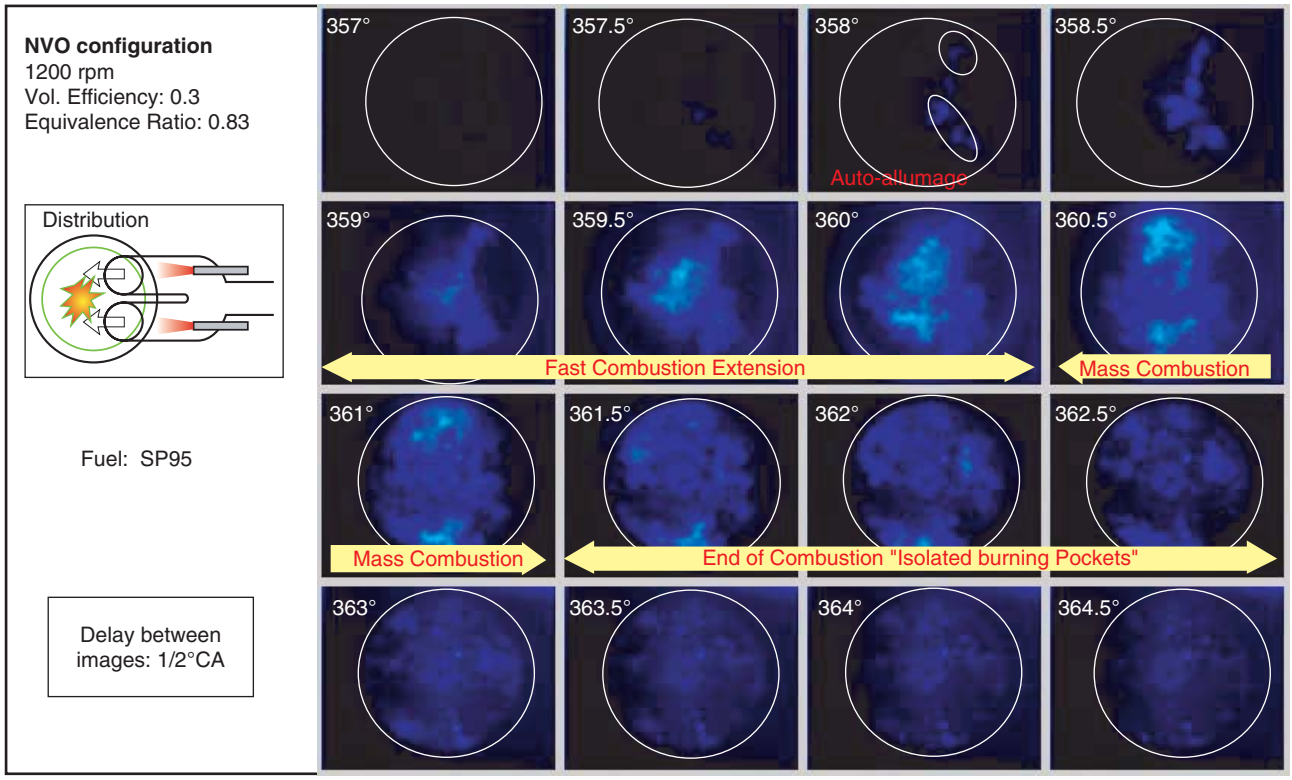

Figure 11

Temporal evolution of the combustion process imaged by direct observation of the chemiluminescence emission - NVO configuration, symmetric injection.

mode and NVO valve configuration. Detailed observation of this sequence and more than 150 similar ones provided the following insights on the CAI combustion process:

1. Combustion starts with localized auto-ignition. Multiple auto-ignition sites, which are identifies as the first detectable reaction zones, may appear simultaneously.
2. Comparatively to spark-ignited combustion (see *Fig. 12*), the edge of reaction zones observed in CAI running conditions display a gradual decay of the combustion light intensity going from the inside of the burning zones to the fresh mixture. The chemiluminescence intensity being representative of the local reaction rate and the height of the reaction zone along the observation axis, the low spatial intensity gradient observed at the border of the combusting areas indicates that:
   – The reaction rate is highest in the center of the observed burning zones and gradually decreases toward the borders.
   – The height/thickness of the reaction zone is larger in the center than on the sides.

   These results tend to show that CAI combustion is characterized by oxidation reactions taking place in large volumes. In comparison, in standard spark-ignited combustion, the reaction zone is confined to the thickness of the flame which defines the limit between burned gases and fresh mixture.
3. Looking at Figure 11 in the border area of the main reaction zones, it can be observed that the local chemiluminescence intensity first increases over a few crank angle degrees (from 358.5 to 360°CA). This evolution of the combustion light intensity can be interpreted as a local acceleration of the oxidation reactions. Looking at the center of the combustion chamber between 358.5 and 362°CA, the evolution of the local chemiluminescence intensity shows that the complete oxidation of the fresh mixture takes about 3 to 4°CA. During this period, first the combustion light appears as the mixture auto-ignites. Then, the chemiluminescence intensity becomes more intense as the reaction rate and thus the local heat release rate increases. Eventually, the combustion light intensity decays showing that the oxidation of the fresh mixture is being completed. Overall, it can be concluded that in CAI combustion the time scale associated with the chemical reaction process is in the order of a few crank angle degrees (observation done at 1200 rpm). In comparison, in spark-ignited engines where the combustion is characterized by a propagating flame, the chemical time scale is infinitely small compare to the engine rotation period.

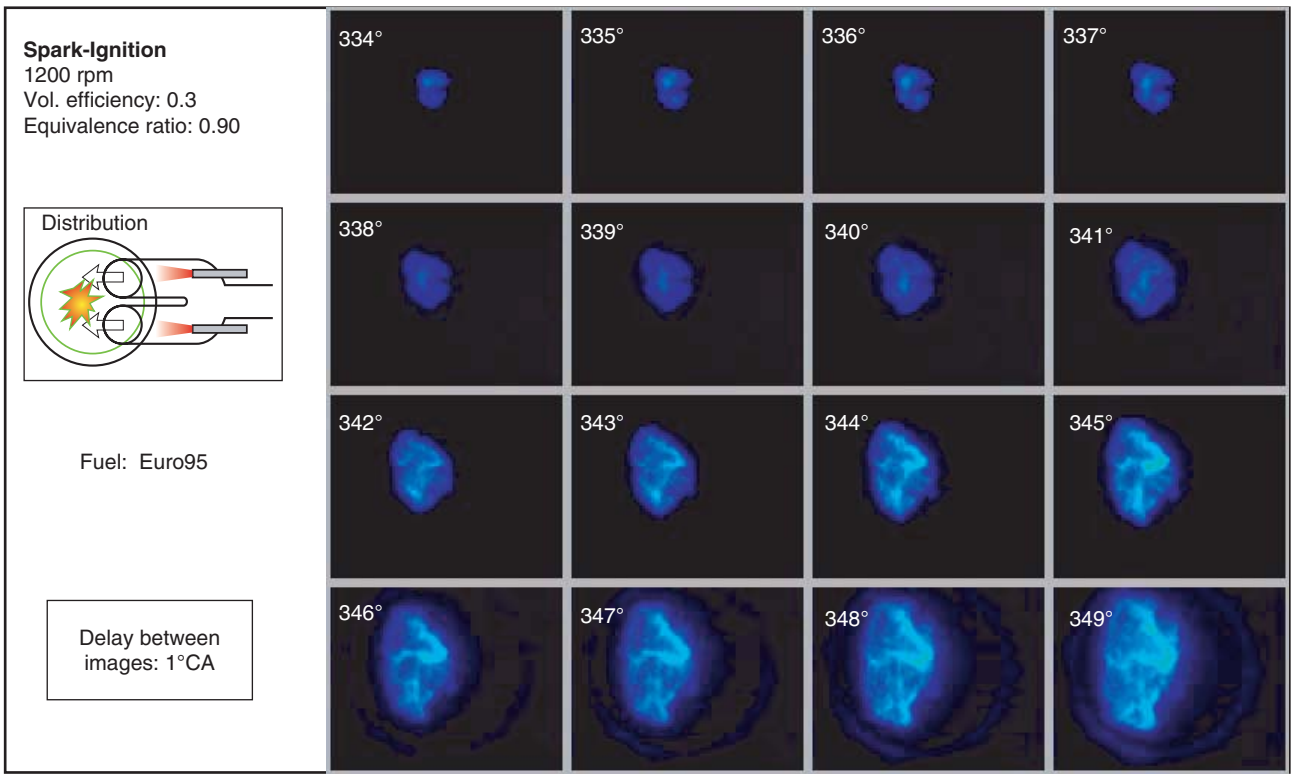

Figure 12

Temporal evolution of the combustion process imaged by direct observation of the chemiluminescence emission - Spark ignition operation.

4. In CAI mode, the extension of the combustion zone is characterized by the initiation of oxidation reactions in the fresh mixture bordering the initial combustion zones. On the chemiluminescence images the auto-igniting areas can be detected through the appearance of low intensity light emission. The extension mechanism can be described as a continuous auto-ignition process resulting in a succession of local combustion events. This is clearly illustrated by comparing in Figure 11 the images acquired at 360° and 362°CA. The area of the combustion chamber occupied by burning gases at 360°CA appears at 362°CA as a dark zone where the combustion is completed. The peripheral regions which do not exhibits chemiluminescence emission at 360°CA clearly appears as combusting areas at 362°CA. In comparison, in SI mode the combustion process is characterized by a flame propagation process resulting in a homothetic growth of the burned gas volume delimited by the flame (see *Fig. 12*).

5. While the beginning of the combustion process is characterized by close reaction zones mostly concentrated in the middle of the combustion chamber, the end of the combustion process clearly exhibits multiple burning pockets located on the border of the observed area. In the peripheral area located near the cylinder liner and the pentroof axis of the cylinder head, the extended piston does not permit observation within approximately 7 mm of the cylinder walls and thus limit the access to the border of the combustion chamber volume. However, in the vicinity of squish zones the piston window allows a full optical access to the border of the pentroof combustion chamber and therefore to the gas layer located near the walls of the chamber. Consequently, it may be concluded that the observation of combustion zones preferentially located on the sides of the viewing area at the end of the heat release process indicates that the combustion ends on the borders of the combustion chamber. This observation very probably implies that the combustion first starts in the middle of the combustion chamber where the fresh mixture which is less affected by heat loss to the walls exhibits a shorter ignition delay. Then, by successive auto-ignitions, the combustion zone moves toward the thermal boundary layer next to the cylinder walls.

6. The combination of a chemical time scale of several crank angle degrees and the fast combustion extension process allows for the existence of a “mass-combustion” phase during which oxidation reactions occur simultaneously in the whole volume of the combustion chamber. Due to the large quantity of fresh mixture simultaneously burning,

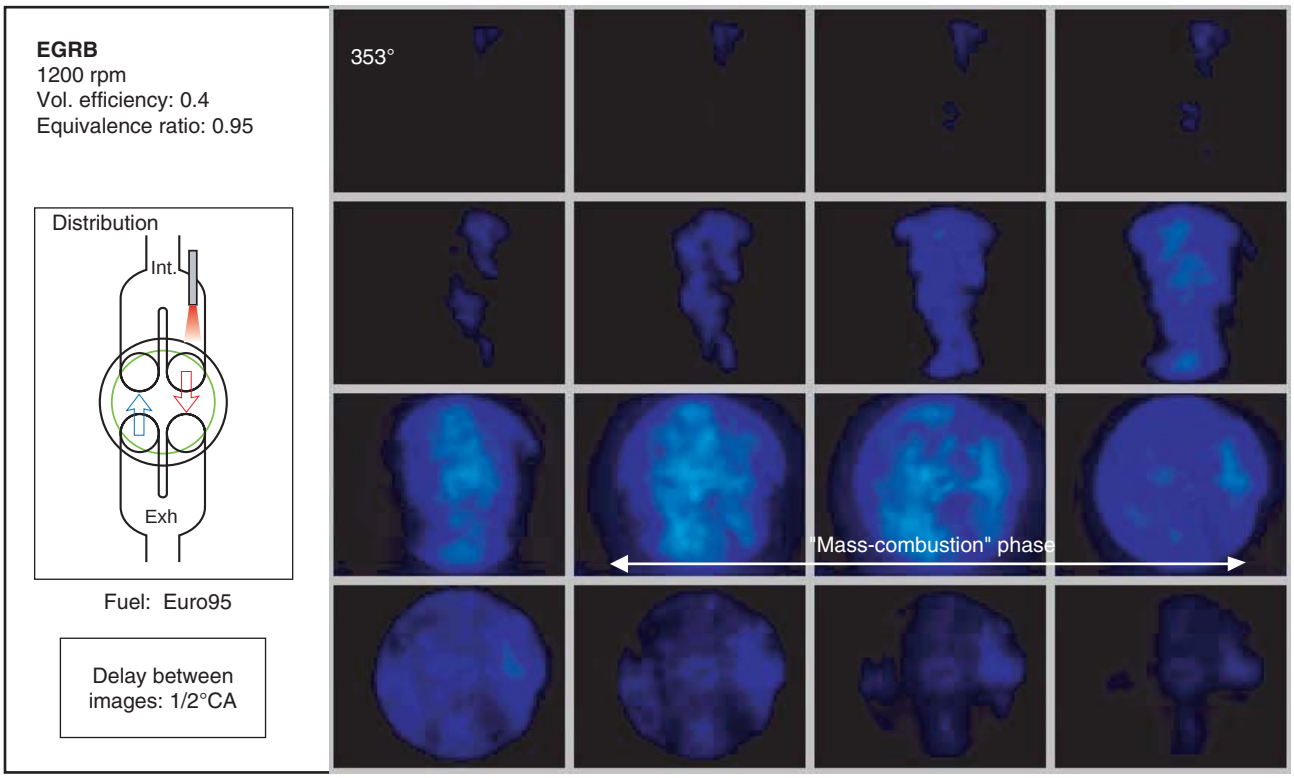

Figure 13

Temporal evolution of the combustion process imaged by direct observation of the chemiluminescence emission - EGRB configuration.

this phase is believed to be characterized by high heat release rate. In the image sequence of Figure 11, the "mass-combustion" phase lasts less than one crank angle degree and can be identified at 361°CA. A much longer homogeneous combustion phase can be observed in Figure 13 showing the temporal evolution of the combustion process in EGRB configuration. The occurrence of a "mass-combustion" phase requires a fast extension of combustion process. Therefore, it is favored by fairly uniform ignition delay thorough the combustion chamber and thus homogeneous temperature and equivalence ratio fields. During this phase, the global heat release rate is controlled by the oxidation reaction rate and is thus greatly affected by the dilution rate.

2.2 Combustion in EGRB Configuration

Observation of Figure 13 which displays an example of the temporal evolution of the combustion phase imaged in EGRB configuration shows a combustion process very similar to the one analyzed in NVO configuration. The main differences are:

– In EGRB configuration, the "mass-combustion" phase represents a significant part of the combustion process. A quasi uniform chemiluminescence emission can be observed in the whole combustion chamber during about 2°CA.
– The end of the combustion process does not exhibit a clear phase with isolated reacting zones located in the periphery of the viewing area. Instead, it appears than the combustion process rather suddenly stop after the homogeneous combustion phase.

These observations corroborate with the burned-mass fraction curved computed from the cylinder pressure trace. As shown in Figure 14, the end of the combustion is characterized by a slow decay of the heat release rate in NVO configuration and a sudden stop of the heat release process in EGRB configuration. The differences observed in the shape of the heat release rate in NVO and EGRB configurations may have two origins. First of all, the different valve actuation strategies may result in a more homogeneous air/fuel/residual gas mixture in the EGRB configuration. Secondly, the chosen EGRB strategy significantly shorten the auto-ignition delay (see *Fig. 14*) resulting in a advanced combustion phasing, which may contribute to increase the pressure-rise rate and to the more rapid end of the heat release process.

2.3 Formation of Auto-Ignition Precursors

While direct visualization allows detection of combustion chemiluminescence emission which only exists during the heat release period, LIF imaging of auto-ignition precursors such as formaldehyde may be used to detect and investigate the fuel decomposition process preceding the main combustion phase. In this work, the previously described LIF355 technique was used to detect formaldehyde and follow the evolution of formaldehyde concentration in the combustion chamber. As shown in Figure 15, CH_2O which results from the thermal decomposition of the fuel is first detected around 340°CA. From the evolution of the average LIF355 signal, it can be deduced that the production rate of formaldehyde increases until the concentration of CH_2O reaches a maximum just prior to auto-ignition. Once auto-ignition has started, formaldehyde is very rapidly consumed. The rate at which CH_2O is locally consumed may be visually evaluated from the image shown in Figure 15 which was acquired just after the appearance of the first auto-ignition

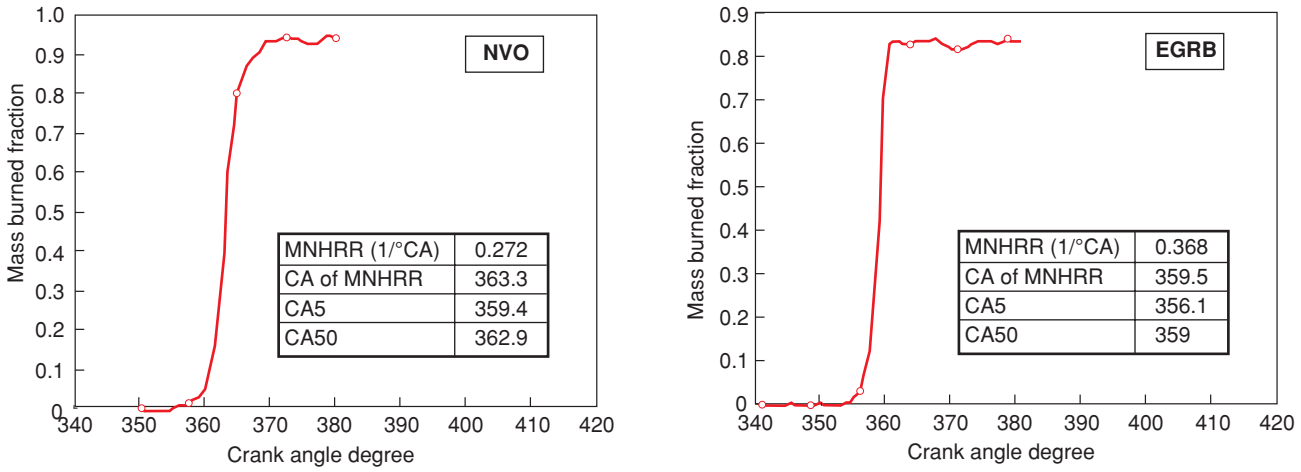

Figure 14

Results of heat-release analysis based on cylinder pressure trace (MNHRR: Maximum Normalized Heat Release Rate).

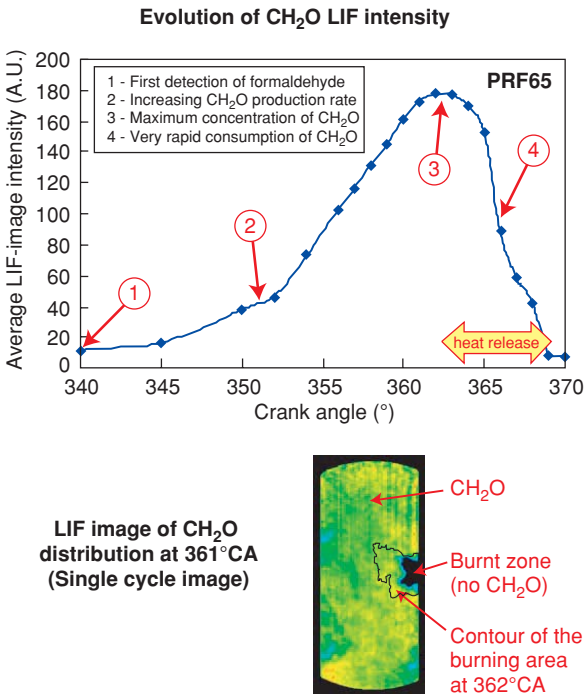

Figure 15

Evolution of the formaldehyde concentration in the combustion chamber during the pre-auto-ignition phase, analyzed via 355-nm LIF imaging. NVO configuration, 1200 rpm, equivalence ratio 0.3, vol. efficiency 0.9.

site. This image exhibits the CH_2O distribution, clearly showing the initial reaction zone which corresponds to the area where CH_2O was consumed and the contour of the reaction area detected one crank angle degree later in the same cycle. It clearly appears that locally CH_2O is totally consumed in less than one crank angle degree. In comparison, about 20°CA are necessary to reach the maximum CH_2O concentration during the precursors production phase.

Based on the detection of formaldehyde, it can be concluded that in the tested CAI configuration there is a 20°CA period preceding the onset of heat release during which fuel is being decomposed into auto-ignition precursors such as formaldehyde. During this 20°CA period, no heat release was detected from the cylinder pressure analysis. Accordingly, this fuel decomposition stage may not be associated with cool flames which are typically observed in diesel HCCI engines [30].

2.4 Nature of CAI Combustion

Summarizing the previously discussed observations, the CAI combustion process can be described as a five steps mechanism:

1. Formation of auto-ignition precursors (thermal decomposition of the fuel).
2. Local ignition of the fresh mixture. Auto-ignition may occur simultaneously in several locations.
3. Fast extension of the combustion throughout the chamber. The extension mechanism is characterized by successive auto-ignitions in the areas bordering the initial combustion zones. The continuous initiation of oxidation reactions in neighboring regions results from the global temperature increase caused by the pressure rise, which is itself induced by the on-going heat release.
4. "Mass-combustion" phase. During this phase oxidation reactions occur simultaneously in the whole volume of the combustion chamber. Excessively high heat release rate may be expected.
5. End of combustion characterized by isolated reaction zones preferably located close to the cylinder walls (in NVO configuration).

Concerning the structure of CAI combustion zones, comparatively to SI combustion (see *Fig. 16*), two main characteristics may be emphasized:

– In CAI operation oxidation reactions occur simultaneously in a large gas volumes. The differences in size and location of the reaction zones revealed by direct observation of the combustion process in SI and CAI operation were emphasized by OH radical images. A LIF OH image provides a 2D cross sectional view of the combustion gases, revealing the OH production areas which correspond to the reaction zones. Figure 17 shows LIF OH images acquired during SI and CAI operation. In SI configuration, OH images clearly show the burned gas area characterized by a fairly uniform OH distribution. The burned gas zone is bordered by a thin zone of high OH concentration (strong LIF signal) revealing the existence of a confined OH production zone which corresponds to the flame front. In CAI configuration, the OH distribution is characterized by spatially separated pockets with uniform OH distribution and a absence of preferential zone of production.

– The chemical kinetic time scale associated with the oxidation reaction is in the order of a few crank angle degrees in CAI operation. Comparatively to SI combustion, in CAI combustion the local chemical reaction rate is relatively slow.

In CAI operation the high global heat release rate results from the summation over a large volume of reacting gases of local heat releases of moderate amplitude.

Regarding the control of the rate of heat release, two key parameters were identified:

– The volume of gases simultaneously reacting: the quantity of the fresh mixture which reaches auto-ignition conditions at anytime depends on the initial mixture quality. In particular, managing the homogeneity of the equivalence ratio and/or the temperature field may offer a mean of combustion rate control.

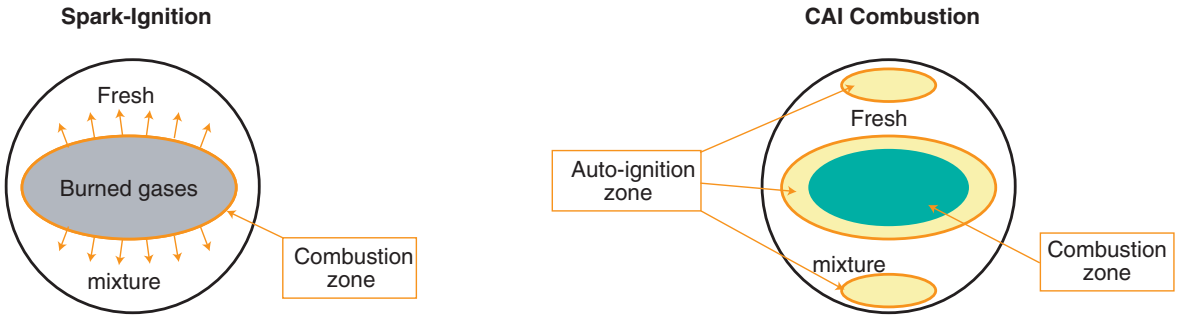

Confined combustion zone:
flame thickness ~0.1 mm

Chemical time scale << 1°CA.

Combustion propagation
(Conduction/Diffusion/Turbulence)
→ Flame speed: ~ 10 m/s

Combustion duration: ~ 30-40 °CA

"Mass-combustion": large volume of reacting gases

Chemical time scale ~ 2-3 °CA
→ High heat release rate

Combustion duration: ~4-7°CA

Figure 16

Structure and main characteristics of CAI combustion.

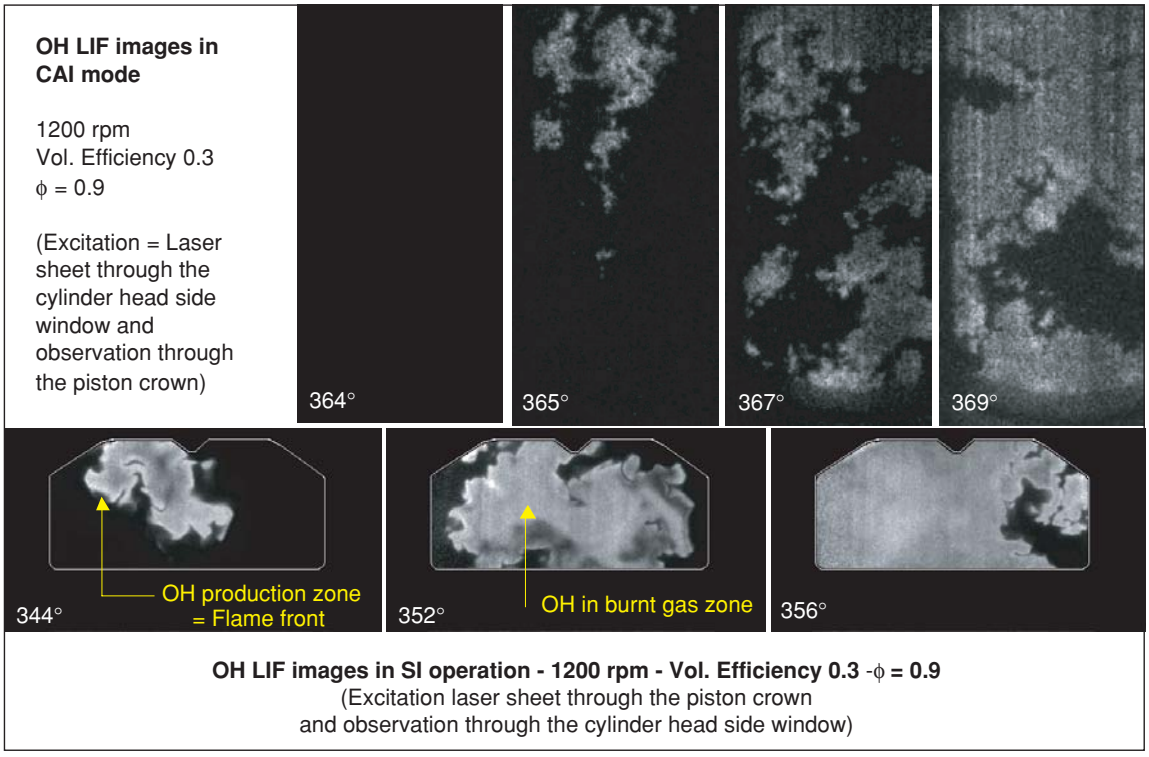

Figure 17

Comparison of OH-LIF images of the structure of the combustion zone in SI and CAI operation.

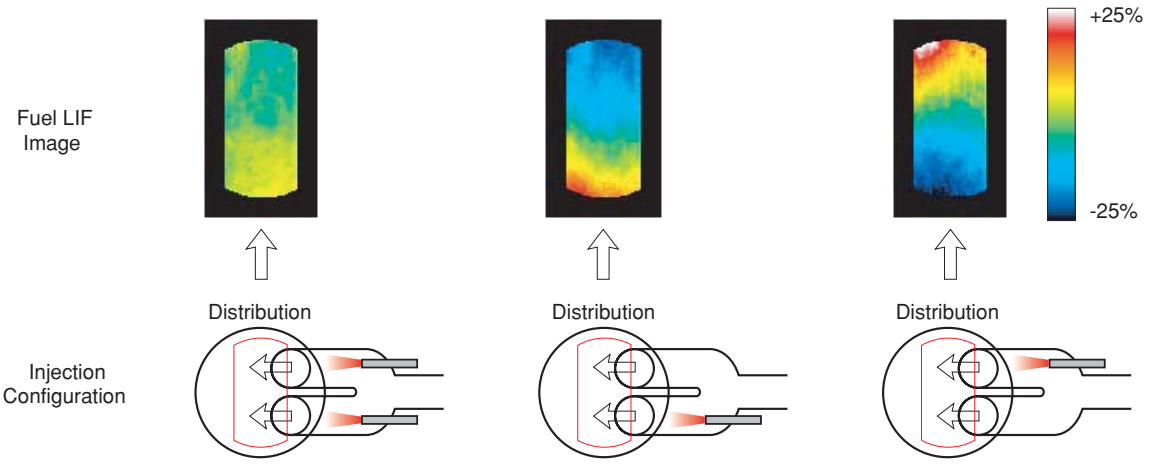

Figure 18

Fuel distribution observed by LIF imaging in various injection configurations. 1200 rpm, Vol. efficiency 0.3, Equivalence ratio 0.83. Color scale: –25% to +25% of the mean fuel concentration.

– The chemical reaction rate: the rate at which complete oxidation is achieved is very dependant on the rate of dilution by burned gas and air. Both, the amount of recycled burned gas and the equivalence ratio may be tentatively used to control the rate of heat release.

3 MIXTURE QUALITY EFFECTS

3.1 Air/Fuel Ratio Distribution

3.1.1 Fuel Stratification via Port Fuel Injection

In order to study the effect of inhomogeneous fuel distribution on the combustion process, a stratification of the fuel concentration was generated by non-symmetric port fuel injection. As shown in Figure 18, the deactivation of the injection in one of the two intake ports creates a stratified fuel distribution in the combustion chamber. On the active-injector side the fresh mixture is about 25% richer than the mean equivalence ratio, while the opposite side is about 25% leaner. These results are based on 200-cycle averaged LIF images of the fuel concentration. The effect of such fuel distribution can be seen on Figure 19 where the location of the centers of combustion zones detected in the early stage of combustion are plotted for 200 consecutive cycles in each of the three tested injection configurations. While in the case of symmetric injection, the auto-ignition zones appear to be almost homogeneously distributed along the pentroof axis of the combustion chamber, in the case of non-symmetric injection the initial reaction zones are preferably located on the side of the active injector and thus in the richer area of the combustion chamber. Considering the crank angle of 5% burned mass, it appears that the fuel stratification generated

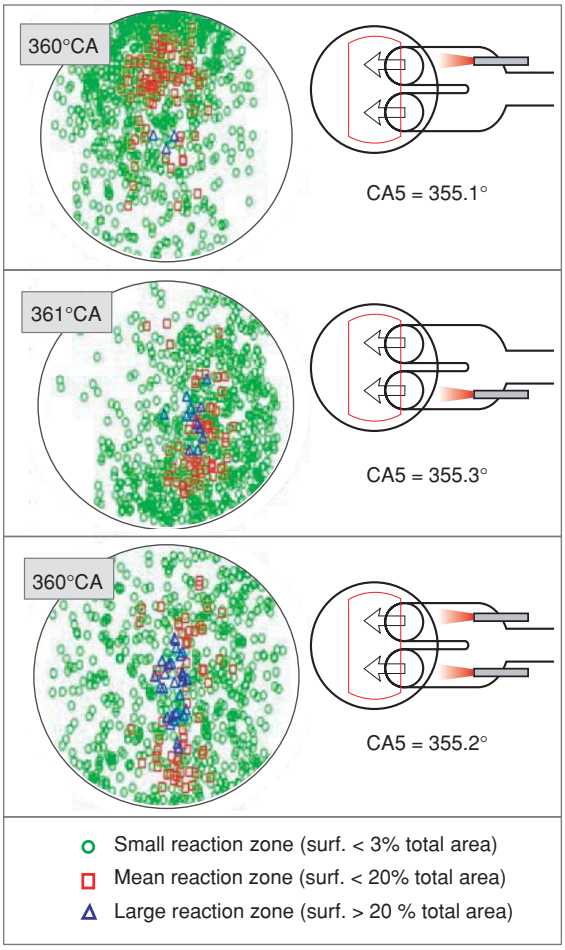

Figure 19

Statistical distribution (200 cycles) of the first reaction zones observed in various injection configurations.

by non-symmetric port fuel injection does not significantly affect the combustion phasing.

3.1.2 Fuel Inhomogeneities Effect

A high speed intensified CCD camera (USS LaVision) was used to generate within a single engine cycle one LIF image of the fuel distribution and 15 images of the combustion chemiluminescence emission. The direct-observation images were used to detect the initial stage of combustion and identify contours of the first reaction zones. Figure 20 shows eight examples of LIF fuel distribution images on which are superimposed contours of the initial reaction zones detected in the same cycle. Because of laser absorption by combustion precursors issued from fuel decomposition, no LIF observation could be performed in the compression stroke after 340°CA. Consequently, the fuel LIF images were acquired at 340°CA while the combustion observations and in particular the auto-ignition sites detection were conducted between 355 and 360°CA. In order to emphasize the fuel distribution inhomogeneities, the color scale limits of the LIF images was set to plus and minus 25% of the average LIF signal in the image. As seen in Figure 20, the amplitude of the detected inhomogeneities in the fuel field is about 20% of the average fuel concentration in the case of symmetric port injection. Moreover, the positions of the fuel inhomogeneities seems to vary randomly from cycle to cycle. This later result is confirmed by the fact that 200 cycle-averaged fuel field images shows a fully homogeneous fuel distribution *(Fig. 18)*. In order, to detect an eventual correlation between the fuel inhomogeneities locations and the positions of the initial reaction zones the single-cycle double observations were conducted over 50 consecutive cycles and the following histograms were compared:

- Histogram of the equivalence ratio distribution within the fuel distribution LIF image.
- Histogram of the initial reaction zones distribution as a function of the average equivalence ratio observed at 340°CA within the contours of the reaction zones detected at the beginning of the combustion process (355 ~ 360°CA).

Histograms of the equivalence ratio field and of the auto-ignition sites distribution are plotted in Figure 21 for the symmetric injection configuration and in Figure 23 for the non-symmetric injection case. When comparing the histograms, a net correlation between the richer or the leaner areas and the locations of the initial reaction zones would be indicated by a shift of the auto-ignition sites distribution on respectively the richer or the leaner side of the mean fuel distribution. It is important to mention that the sensitivity of this method to identify any existing correlation between the fuel/air mixture quality and the location of the initial reaction zones may be altered due to the following aspects of the experimental approach:

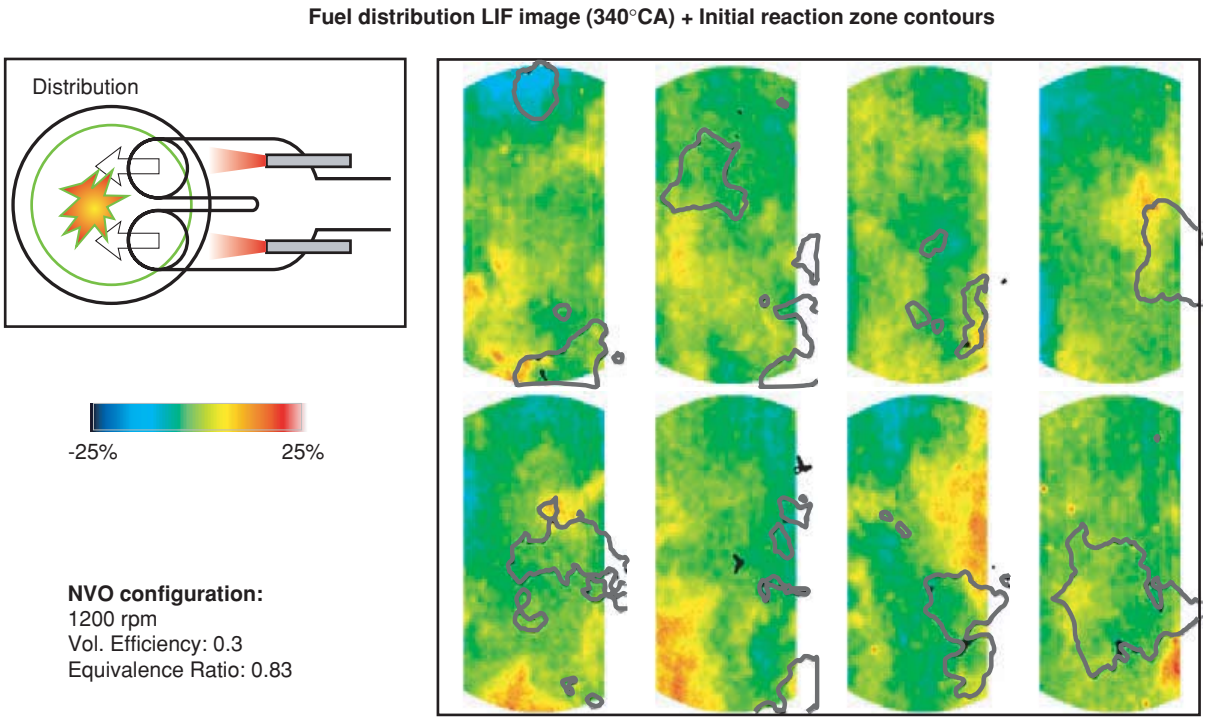

Figure 20

Examples of fuel distribution LIF images and initial reaction zones observed in the same cycle. Symmetric port injection.

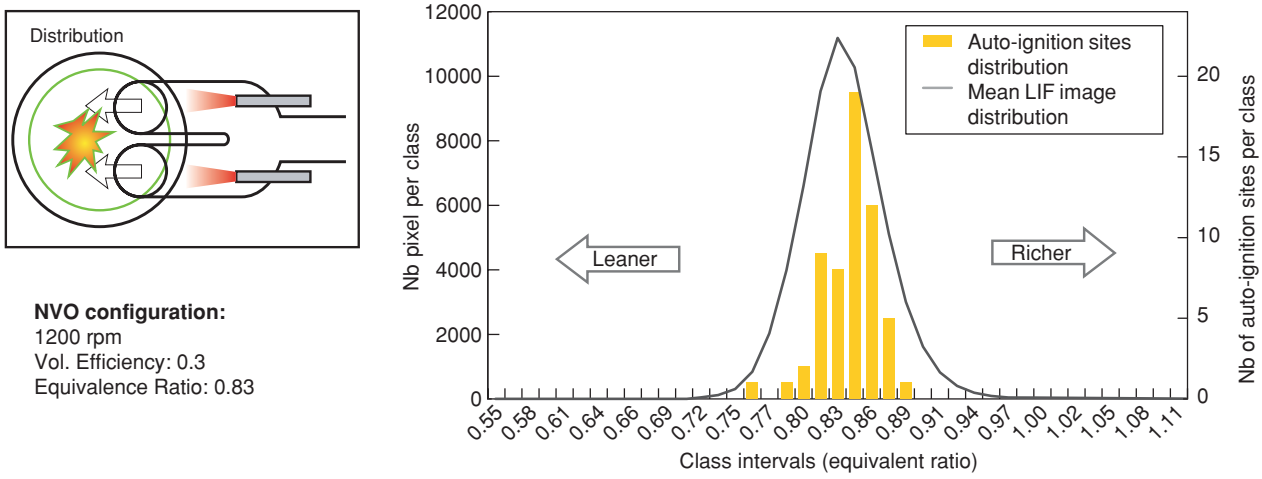

Figure 21

Histogram of the auto-ignition sites repartition as function of the local equivalence ratio. Symmetric port injection.

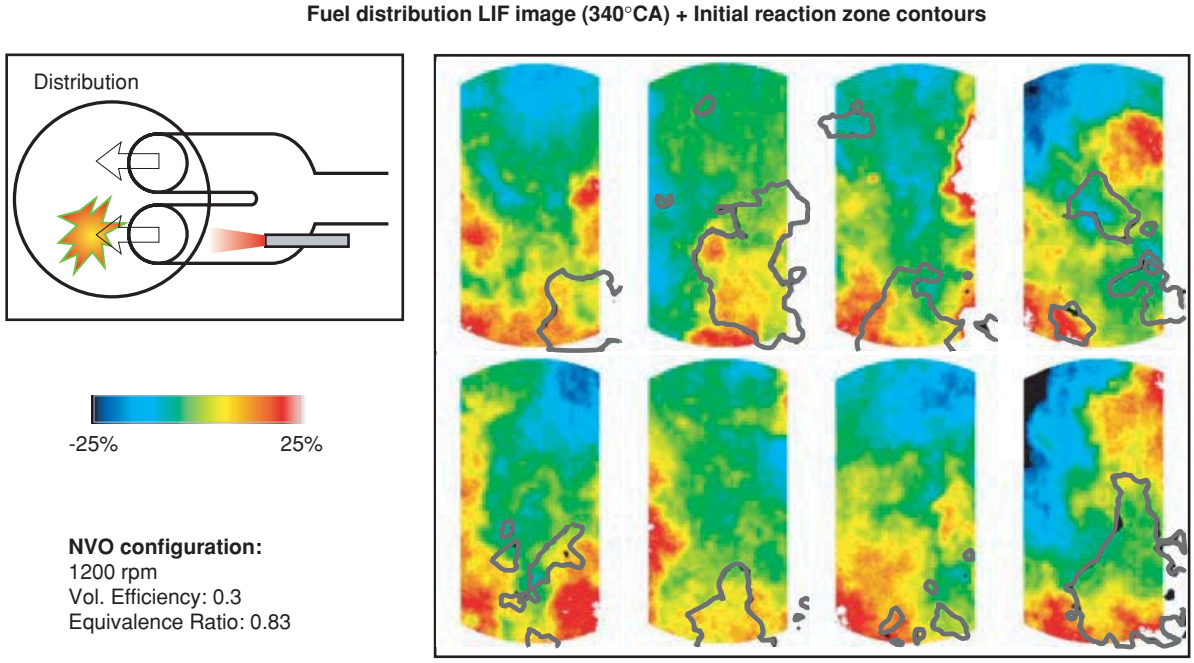

Figure 22

Examples of fuel distribution LIF images and initial reaction zones observed in the same cycle. Non-symmetric port injection.

– The fuel heterogeneities are observed in a horizontal plane corresponding to the laser sheet excitation while the first reaction zones are detected by direct observation and thus in the whole volume of the combustion chamber.
– Because of the time delay between the fuel field observation (340°CA) and the detection of the first reaction zones (355 ~ 360°CA), the quality of the air/fuel mixture and the position of the fuel field inhomogeneities may be modified between the two observations to be correlated.
– In order to limit the amount of data, the observations were limited to 50 consecutive cycles. Moreover, the number of acquisitions relevant for the statistical analysis was reduced when initial reaction zones were detected outside the fuel field observation plane defined by the laser sheet.

In Figure 21, the slight shift of the auto-ignition sites histogram toward the richer side tends to indicate that combustion preferably starts in the richer fuel inhomogeneities. This result obtained in the symmetric injection

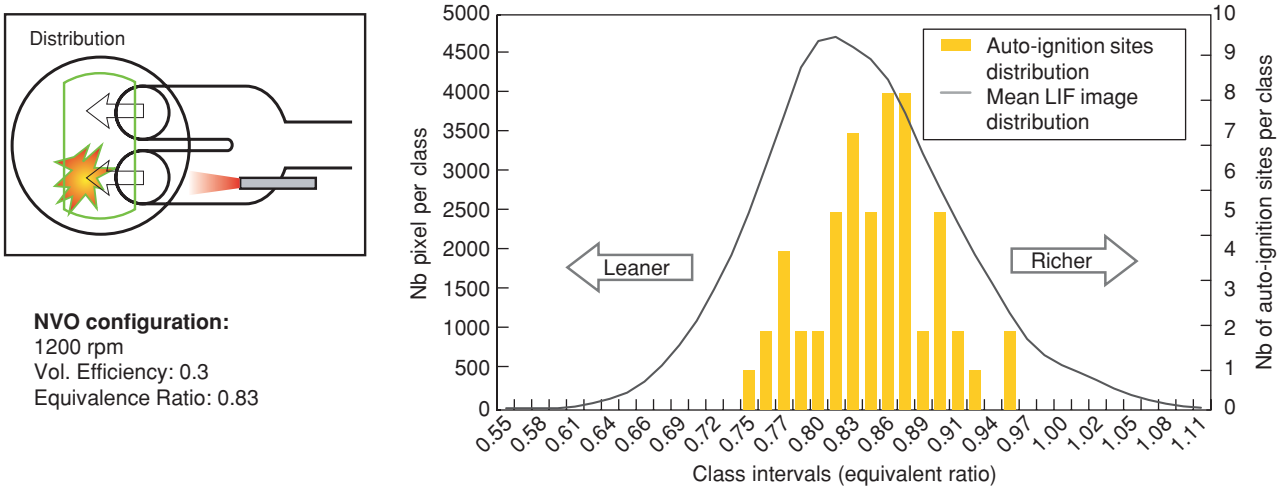

Figure 23

Histogram of the auto-ignition sites repartition as function of the local equivalence ratio. Non-symmetric port injection.

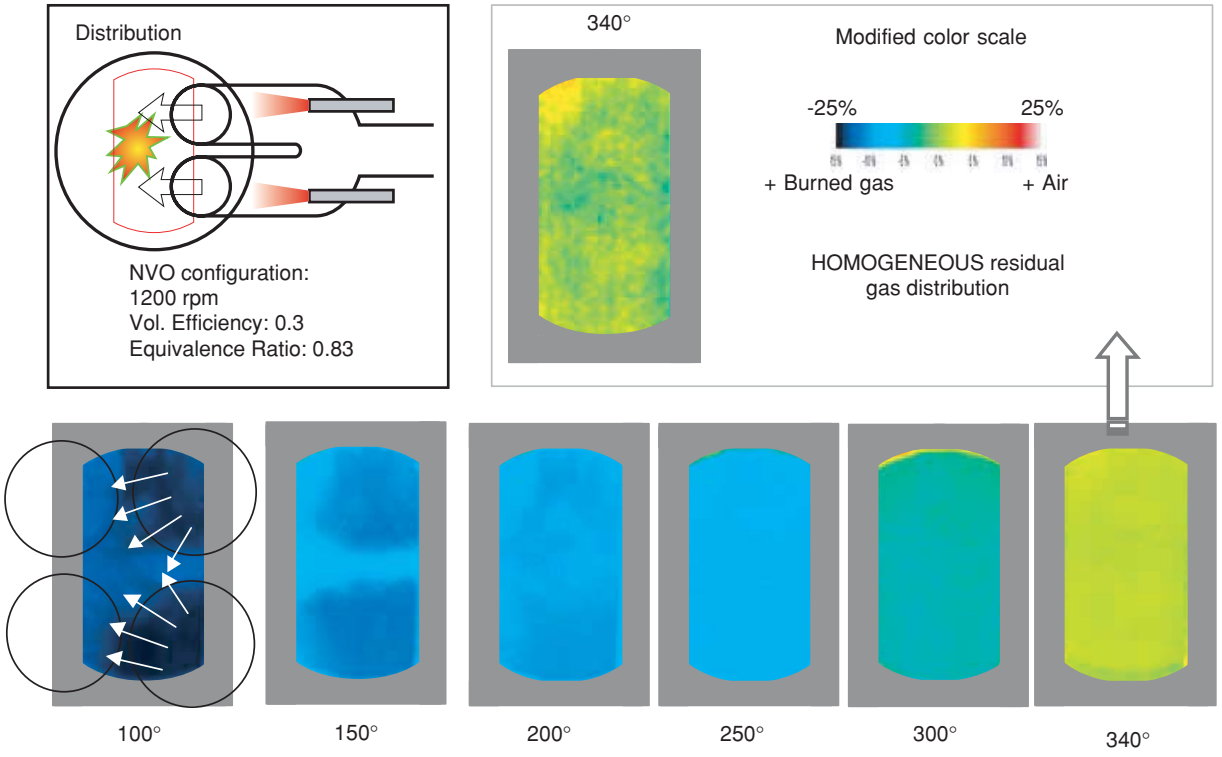

Figure 24

Temporal evolution of the averaged (over 200 consecutive cycles) residual gas distribution observed by LIF imaging. NVO configuration, two active intake valves.

configuration, where the shift between the fuel distribution histogram and the initial reaction zone histogram is small, is confirmed by the observations obtained in the non-symmetric port injection. As shown in Figure 22, when fuel is injected in only one intake port, the fuel concentration inhomogeneities are of larger amplitude, about 30% of the average fuel concentration. In these conditions where the overall fuel field is much more heterogeneous, as indicated by the larger histogram of the fuel distribution (see *Fig. 23*), the shift of the auto-ignition sites histogram toward the richer side of the fuel distribution histogram is much more significant. Consequently, it can be concluded that a clear correlation exists between the air/fuel mixture and the location of the auto-ignition sites and that the initial reaction zones preferably appear in the richer areas of the combustion chamber. Accordingly, the cycle to cycle variations of the initial reaction zone positions can be at least partly attributed to the existence of fuel concentration inhomogeneities whose position fluctuates from one cycle to another.

3.2 Residual Gas/Air Mixture Quality

The purpose of the work described in the following section was to study the residual gas/air mixing process and to investigate the effect of local inhomogeneities on CAI combustion.

3.2.1 Average Residual Gas Distribution

The quality of the air/residual gas mixture was investigated using LIF imaging based on fresh air acetone seeding. In order to suppress the contribution of cycle to cycle fluctuations of the residual gas distribution and thus to enable the detection of small amplitude and large scale stratifications, the analysis was conducted on 200-cycle averaged images.

Figure 24 shows the evolution of the mixing process between the fresh air and the residual gases during the intake and compression strokes. Because the tracer is mixed with the fresh air, the dark area are rich in residual gas and the bright ones (toward red and white in the color scale) are rich in fresh air. On the images acquired at 100 and 150°CA, the fresh air entering the combustion chamber can clearly be observed at the periphery of the intake valves. LIF images acquired after 200°CA shows that the air/residual gas mixture quickly becomes homogeneous. The increase of the average LIF signal intensity during compression stroke (between 200 and 340°CA) is a consequence of the increasing density. In order to emphasize any stratification of the mixture, the color scale of the average image obtained at 340°CA was modified so that the limit of the color scale correspond to plus and minus 25% of the average LIF signal in the image. As shown in Figure 24, even with the modified color scale the air/residual gas mixture appears to be fully homogeneous at 340°CA. The very small variations in the LIF intensity are smaller than 5% and correspond to the limits of the optical technique. Moreover, because the temperature dependence of acetone quantum efficiency amplifies the sensitivity of the technique, it can be concluded that no repeatable large scale inhomogeneities of the residual gas distribution exists in the observation plane. This result was confirmed by 3D simulation of the exchange and compression strokes. In fact in the NVO configuration with two active intake valves, the simulation results showed that the residual gas distribution and thus the temperature field becomes almost homogeneous in the whole volume of the combustion chamber before top dead center of compression stroke.

3.2.2 Residual Gas Inhomogeneities

A procedure similar to the one used to investigate the effect of fuel distribution inhomogeneities on the auto-ignition sites location was used to study the influence of small scale cycle to cycle fluctuations of the residual gas distribution on the location of the initial reaction zones. The analysis was based on residual gas distribution and direct combustion observation imaged within one engine cycle. The experiment was repeated over 50 consecutive cycles. Figure 25 shows eight examples of LIF images of the residual gas distribution acquired at 340°CA on which are superimposed contours of the initial reaction zones detected in the same cycle. From the single-shot images of Figure 25, it can observed that the residual gas distribution is not fully homogeneous. Local inhomogeneities of the air/residual gas mixture exist and their position varies randomly from one cycle to another. The amplitude of the local variations of the LIF intensity signal, which is representative of the local residual gas concentration, are in the order of 15% of the average signal intensity. Because of the temperature sensitivity of acetone quantum efficiency, this result implies that the amplitude of the local inhomogeneities of the residual gas distribution is less than 15% of the average residual gas concentration.

In order to detect an eventual correlation between the residual gas inhomogeneities and the locations of the initial reaction zones, the histogram of the residual gas average distribution and the histogram of the auto-ignition sites distribution were computed. For this analysis, the histogram of auto-ignition sites distribution was computed as a function of the average residual gas content in the area defined by the contour of the detected reaction zones. Looking at Figure 26, it appears that the histogram of auto-ignition sites distribution is slightly shifted toward the areas where the residual gas concentration is higher than average. From this result it can be concluded that the areas with high residual gas concentration tends to be more favorable to the onset of auto-ignition. The authors believed that higher temperature levels encountered in areas rich in residual gas are responsible for accelerating the auto-ignition process. Because the experiment was repeated and identical results were obtained, the analysis based on the comparison of the two histograms is believed to be relevant even though the shift observed is

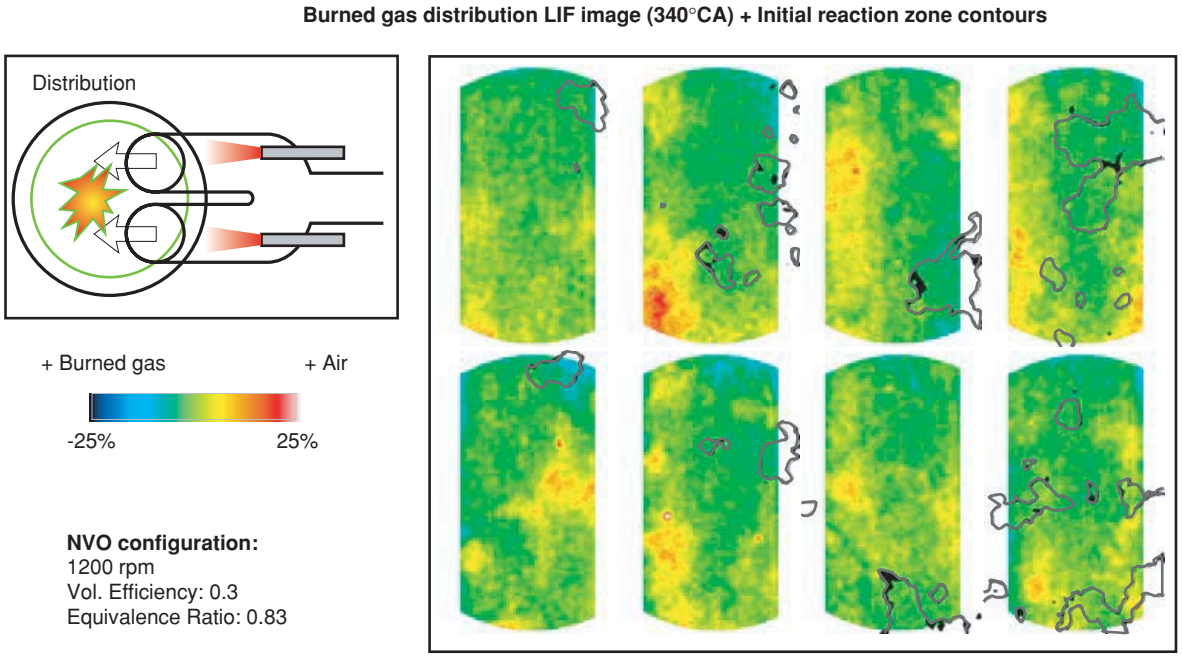

Figure 25

Examples of burned gas distribution LIF images and initial reaction zones observed in the same cycle. Symmetric injection.

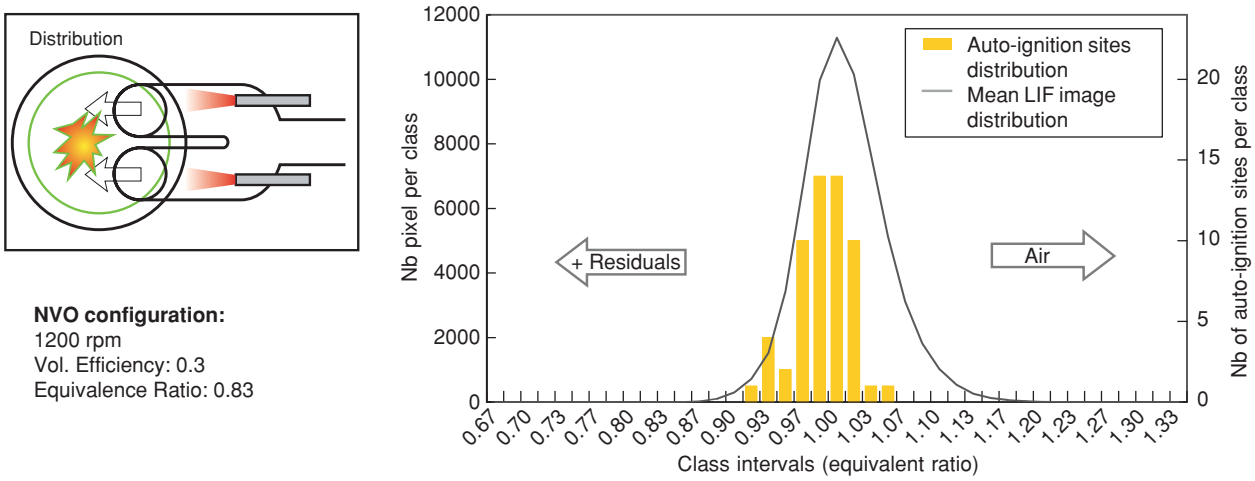

Figure 26

Histogram of the auto-ignition sites distribution as function of the residual gas distribution.

relatively small. As for the correlation analysis of the single-shot fuel distribution and auto-ignition sites locations, the sensitivity of the technique is altered by the time delay between the LIF image acquisition and the onset of the first reaction zones.

Eventually, as fuel rich areas were found to be clearly favorable to auto-ignition and because with port injection areas highly concentrated in residual gas are usually poor in fuel, it is believed that auto-ignition site location results from a compromise between high local equivalence ratio and high local gas temperature. Consequently, auto-ignition should occurs at the border between fuel rich fresh pockets and areas with high burned gas concentration. Overall, comparing experimental results regarding the effect of fuel and residual gas inhomogeneities, the local fuel concentration seems to be the primary factor governing the location of auto-ignition sites.

4 DIRECT INJECTION

The fact that initial reaction zones are preferably located in fuel rich areas shows that the auto-ignition delay is locally reduced in mixture inhomogeneities of higher equivalence

ratio. However, because the fresh mixture in combustion chamber is not fully homogeneous but rather characterized by distributed equivalence ratio inhomogeneities, a strong stratification of the air fuel mixture is required to significantly affect the combustion phasing. Such stratification level could not be obtained with port fuel injection and therefore direct injection appeared as a potential way of influencing CAI combustion process.

4.1 Single Injection Operation

In direct injection configuration a Siemens swirl injector was vertically implemented in the center of the combustion chamber. The injection pressure was set to 70 bar. All direct injection tests were conducted in the NVO configuration. First, single injections were used and the influence of the injection timing on the combustion phasing was investigated. Figure 27 shows the cylinder pressure traces obtained when varying the SOI from 590°CA which correspond to the start of the recompression phase to 240°CA in the early compression stroke. In terms of combustion phasing, the pressure traces can clearly be gathered in two groups:

– For SOI during the early recompression phase (SOI < 700°CA), the combustion is phased early and the crank angle of 5% burned mass is at about 351°CA.
– For SOI during the intake stroke, the combustion starts later and the crank angle of 5% burned mass is at about 359°CA.

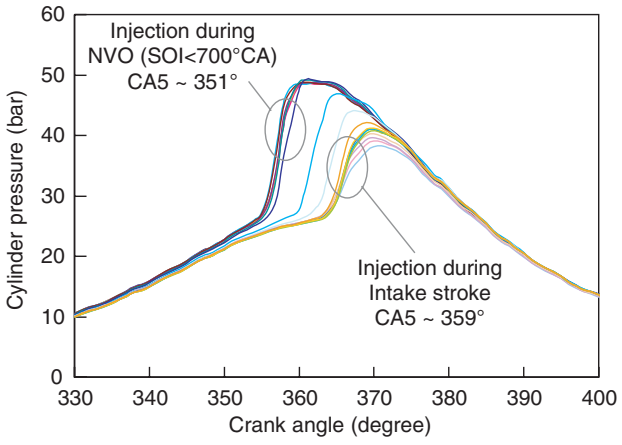

Figure 27

Cylinder pressure traces obtained for various injection phasing. Single direct injection, 1200 rpm, vol. efficiency 0.3, equivalence ratio 0.9.

In fact, it appears that when the injection starts before or at the beginning of the recompression phase, the combustion is phased earlier which indicates that the auto-ignition delay is reduced. Moreover, it should be noticed the highest sensitivity of the combustion phasing to the injection timing is obtained when the SOI occurs during the recompression phase. When injection starts before the recompression or during the intake stroke the combustion phasing is almost unaffected by small change of the injection timing.

A thermodynamic analysis based on the cylinder pressure traces showed that a heat release occurs during the recompression phase when fuel is injected before or during the NVO period and the equivalence ratio measured in the exhaust is below 0.8. The amount of heat release was found to increase with the quantity of remaining oxygen in the burned gases and thus with the excess of air in the fresh mixture. This observation reveals that the combustion of a portion of the injected fuel results in a elevation of the residual gas/air/fuel mixture temperature and consequently shorten the auto-ignition delay in the following cycle. At 0.9 equivalence ratio, the cylinder pressure analysis did not reveal any heat release even though injecting during the NVO phase was found to strongly impact the combustion phasing. It is believed that a partial thermal fuel decomposition occurs during the NVO period and is responsible for shorten auto-ignition delay in the following cycle. Similar results were reported in literature [18, 19, 36, 37].

4.2 Double Injection Operation

In a second step, two double-injection strategies were tested:

1. One injection at the beginning of the intake stroke (SOI 1 = 60°CA) and one injection late in the compression stroke (SOI 2 = 310°CA).
2. One injection at the beginning of the NVO phase (SOI 1 = 650°) and one injection late in the compression stroke (SOI 2 = 310°).

The proportion of fuel injected in each of the two injections was varied from 0 to 100% by step of 25%. In both cases, the global equivalence ratio was 0.74.

In the first injection configuration (see *Fig. 28*), no fuel is introduced before the recompression phase and consequently there is no fuel pre-decomposition or early heat release that may promote auto-ignition in the following cycle. The influence of split injection on the combustion phasing can be seen in Figure 28 which shows the cylinder pressure traces obtained when varying the proportion of fuel in each injection. By comparison with the case where the whole fuel load is introduced at the beginning of intake stroke, it appears that the use of a second injection during the late part of compression stroke significantly reduces the auto-ignition delay, which results in advanced combustion phasing. It is believed that the second injection results in the creation of a rich zone favorable to early auto-ignition and thus responsible for advanced combustion phasing. Moreover, looking at Figure 28, it can be seen that the most advanced combustion phasing is obtained when half of the fuel load is introduced in each of the two injections. In fact, the short auto-ignition delay obtained in the case of 50/50 split

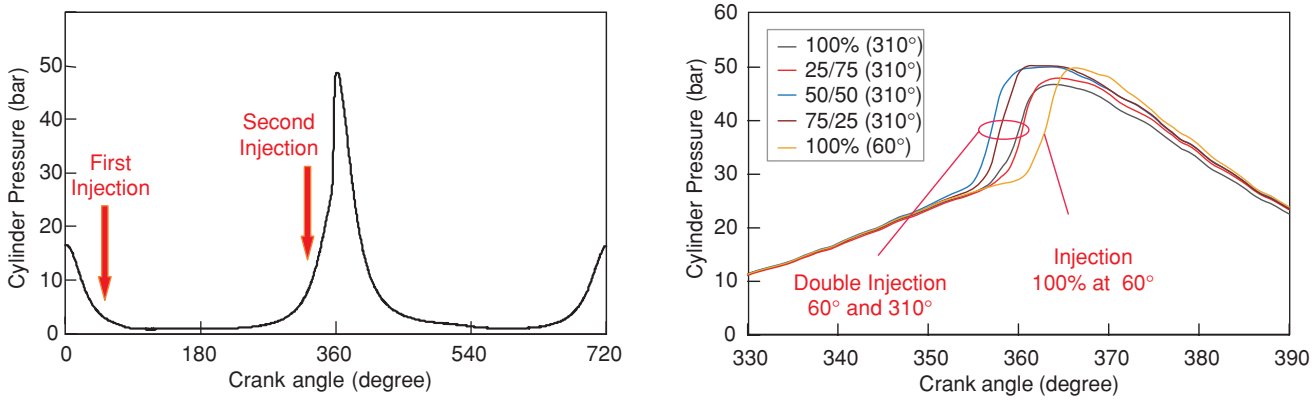

Figure 28

Cylinder pressure traces obtained with double direct injections, first injection at the beginning of the intake phase –1200 rpm, vol. efficiency 0.4, equivalence ratio 0.75.

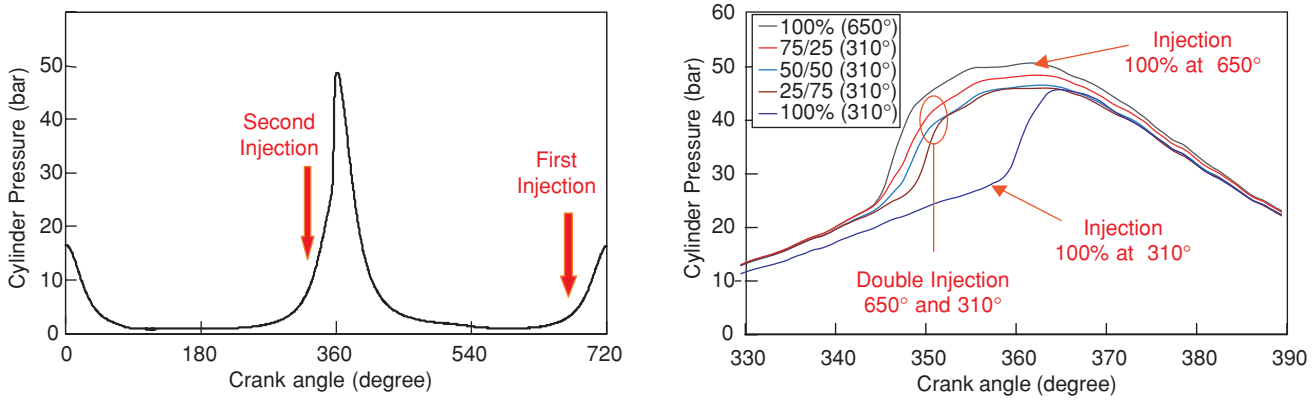

Figure 29

Cylinder pressure traces obtained with double direct injections, first injection at the beginning of the NVO phase –1200 rpm, vol. efficiency 0.4, equivalence ratio 0.75.

injection very probably results from a compromise between the following phenomena:

– The creation of a rich zone which locally promotes auto-ignition.
– The cooling effect of the vaporizing fuel which locally induced a temperature decrease and thus an increase of the auto-ignition delay.

In the second injection configuration (see *Fig. 29*), the cylinder pressure analysis showed the existence of heat release during the NVO period whenever part of the fuel was introduced at the beginning of the recompression phase. Due to this heat release, the combustion phasing was significantly advanced. In fact, among all the tested injection strategies the most advanced combustion phasing was obtained when all the fuel was injected at the beginning of the NVO phase. As shown in Figure 29, when part of the fuel is injected after the recompression phase, auto-ignition in the following cycle is delayed.

Overall, it can be concluded that managing the air/fuel ratio distribution with adequate split direct injections provides a mean of controlling the CAI combustion phasing. As summarized in Figure 30 depending of the timing of injections, three different phenomena may be involved in the determination of the observed auto-ignition delay:

– In the case where oxygen is available in the residual gases and part of the fuel is injected at the beginning of the recompression phase, a pre-decomposition and/or combustion of the fuel occurs and results in an advanced combustion phasing in the following cycle.
– The cooling of the fresh mixture due to the vaporizing fuel tends to delay the combustion start in the case of late injection.
– In case of adequate split injection, the creation of a rich zone favorable to auto-ignition can be used to promote an early combustion phasing.

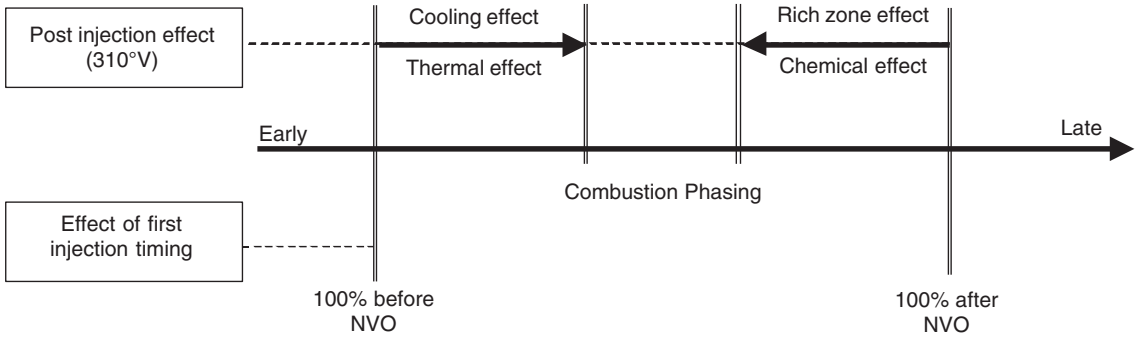

Figure 30

Mechanisms of combustion phasing control by multiple direct injections.

Finally, it should be mentioned that highly stratified regions created with late direct injection may result in NOx and smoke emissions [38].

5 SUMMARY AND CONCLUSIONS

The structure of CAI combustion was investigated using an optically-accessed engine and cycle-resolved direct visualization of the combustion chemiluminescence. The CAI combustion process appeared as a five steps mechanism:

1. Formation of auto-ignition precursors by thermal decomposition of the fuel.
2. Local ignition of the fresh mixture. Auto-ignition may occur simultaneously in several locations.
3. Fast extension of the combustion thorough the combustion chamber. The extension mechanism is characterized by successive auto-ignitions in the areas bordering the initial combustion zones. The continuous initiation of oxidation reactions in neighboring regions results from the global temperature increase caused by the pressure rise, which itself is induced by the on-going heat release.
4. "Mass-combustion" phase. During this phase oxidation reactions occur simultaneously in the whole volume of the combustion chamber. Excessively high heat release rate may be expected.
5. End of combustion characterized by isolated reaction zones preferably located close to the cylinder walls.

Comparing EGRB and NVO configurations through direct visualization and heat release analysis showed that the relative importance of the last two steps may vary significantly from one configuration to another indicating that the air/burned gas mixing process may significantly affect the end of combustion.

A detailed analysis of the CAI combustion zone structure revealed the following characteristics:

– Oxidation reactions occurring simultaneously in large gas volumes.
– Chemical time scale in the order of a few crank angle degrees. Comparatively to SI combustion, in CAI the local chemical reaction rate is relatively slow.
– In CAI mode, the high global heat release rate results from the summation over a large volume of reacting gases of local heat releases of moderate amplitude.

The investigation of the impact of the air/fuel mixture quality on the CAI combustion process showed that:

– Stratification of the air/fuel ratio field obtained with non-symmetric port injection may only affect the location of the auto-ignition sites but not the combustion phasing. Therefore, fuel distribution management offered by port fuel injection can be not be used to influence either the combustion phasing or duration.
– Local fuel-rich inhomogeneities are favorable to auto-ignition and their location correlates well with the position of initial reaction zones.
– The cycle to cycle variations of the auto-ignition sites location is very probably due to fuel concentration inhomogeneities whose position fluctuates randomly from one cycle to another.

The homogeneity of the air/residual gas mixture was investigated using both single cycle and average LIF visualizations. No repeatable large scale residual gas stratification was observed across the combustion chamber. A slight correlation between auto-ignition sites locations and the position of mixture inhomogeneities with high residual gas concentration suggested that in CAI combustion the auto-ignition process is somewhat sensitive to the residual gas distribution.

Because port fuel injection did not offer enough capability to control the in-cylinder air/fuel mixture at the time of auto-ignition, the potential of direct injection for CAI combustion phasing control was evaluated in NVO configuration. Using single injection, CAI combustion phasing was found to be sensitive to the injection timing when injection starts at the beginning of the recompression stroke. In this case, the

pre-decomposition/combustion of a portion of the injected fuel was found to be responsible for reducing the auto-ignition delay in the following cycle. Split injection strategies involving one injection before or after the NVO phase and one during the compression stroke were tested. The late second injection was found to significantly affect the combustion phasing through two opposite effects:

– The cooling of the fresh mixture due to the vaporizing fuel tends to delay the combustion.
– In case of adequate split injection, the creation of a rich zone favorable to auto-ignition locally reduces auto-ignition delay.

Overall, it can be concluded that the potential for air/fuel mixture quality management offered by multiple direct injections can be used to control the phasing of auto-ignition in CAI combustion.

ACKNOWLEDGEMENTS

This work was mostly conducted within the framework of a research program funded by the Groupement Scientifique Moteurs *(GSM-PSA Peugeot Citroën, Renault SA and Institut Français de Pétrole)*. The authors would like to express special thanks to Alexandre Marchal, Thomas Mansion, and Olivier Lafay from Renault, and Thierry Duverger, Elodie Deharte and Erwann Samson from *PSA* for their technical inputs.

REFERENCES

1 Lavy, J., Dabadie, J.C., Angelberger, C., Willand, J., Juretzka, A., Schaflein, J., Lendresse, Y., Satre, A., Schultz, C., Kramer, H., Zhao, L. and Damiano, L. (2000) Innovative Ultra-Low NOx Controlled Auto-Ignition Combustion Process for Gasoline Engines: the 4-SPACE Project. SAE Paper 2000-01-1837.

2 Duret, L. and Lavy, J. (2000) Gasoline Controlled Auto-Ignition (CAI™): Potential and Prospects for Future Automotive Application. IMechE Conference, 21st Century Emissions Technologies, 4-5 December, London.

3 Lavy, J., Dabadie, J.C., Duret, P., Angelberger, C., Le Coz, J.F. and Cherel, J. (2001) Controlled Auto-Ignition (CAI): a Newly Highly Efficient and Near Zero NOx Emissions Combustion Processs for Gasoline Engine Application. IFP International Congress, November 26-27, Editions Technip.

4 Duret, P. (2002) Gasoline CAI and Diesel HCCI: The Way Toward Zero Emission with Major Engine and Fuel Technology Challenges. SAE Paper 2002-32-1787.

5 Zhao, H., Peng, Z., Williams, J. and Ladommatos, N. (2001) Understanding the Effects of Recycled Burnt Gases on the Controlled Autoignition (CAI) Combustion in Four-Stroke Gasoline Engines. SAE Paper 2001-01-3607.

6 Chen, R., Milovanovic, N., Turner, J. and Blundell, D. (2003) The Thermal Effect of Internal Exhaust Gas Recirculation on Controlled Auto Ignition. SAE Paper 2003-01-0751.

7 Zheng, J., Miller, D., Cernansky, N., Liu, D. and Zhang, M. (2003) The Effect of Active Species in Internal EGR on Preignition Reactivity and on Reducing UHC and CO Emissions in Homogeneous Charge Engines. SAE Paper 2003-01-1831.

8 Koopmans, L. and Denbratt, I., (2001) A Four Stroke Camless Engine, Operated in Homogeneous Charge Compression Ignition Mode with Commercial Gasoline. SAE Paper 2001-01-3610.

9 Kaahaaina, N.B., Simon, A.J., Caton, P.A. and Edwards, C.F. (2001) Use of Dynamic Valving to Achieve Residual-Affected Combustion. SAE Paper 2001-01-0549.

10 Fuerhapter, A., Unger, E., Piock, W.F. and Fraidl, G.K. (2004) The New AVL CSI Engine - HCCI Operation on a Multi Cylinder Gasoline Engine. SAE Paper 2004-01-0551.

11 Martinez-Frias, J., Aceves, S.M., Flowers, D., Smith, R. and Dibble, R. (2000) HCCI Engine Control by Thermal Management. SAE Paper 2000-01-2869.

12 Yang, J., Cupl, T. and Kenney, T. (2002) Development of a Gasoline Engine System Using HCCI Technology - The Concept and the Test Results. SAE Paper 2002-01-2832.

13 Persson, H., Agrell, M., Olsson, J.O. and Johansson, B. (2004) The Effect of Intake Temperature on HCCI Operation Using Negative Valve Overlap. SAE Paper 2004-01-0944.

14 Haraldsson, G., Tunestal, P. and Johansson, B. (2003) HCCI Combustion Phasing with Closed-Loop Combustion Control Using Variable Compression Ratio in a Multi Cylinder Engine. SAE Paper 2003-01-1830.

15 Haraldsson, G., Tunestal, P., Johansson, B. and Hyvönen, J. (2002) HCCI Combustion Phasing in a Multi Cylinder Engine Using Variable Compression Ratio. SAE Paper 2002-01-2858.

16 Chen, Z. and Mitsuru, K. (2003) How to Put the HCCI Engine to Practical Use: Control the Ignition Timing by Compression Ratio and Increase the Power Output by Supercharge. SAE Paper 2003-01-1832.

17 Urata, Y., Awasaka, M., Takanashi, J., Kakinuma, T., Hakozaki, T. and Umemoto, A. (2004) A Study of Gasoline-Fuelled Engine Equipped with an Electromagnetic Valve Train. SAE Paper 2004-01-1898.

18 Urushihara, T., Hiraya, K., Kakuhou, A. and Teruyuki, I. (2003) Expansion of HCCI Operating Region by the Combination of Direct Fuel Injection, Negative Valve Overlap and Internal Fuel Reformation. SAE Paper 2003-01-0749.

19 Deschamps, B., Snyder, R. and Baritaud, T. (1994) Effect of Flow and Gasoline Stratification on Combustion in a 4-valve SI Engine. SAE Paper 941993.

20 Hultqvist, A., Christensen, M., Johansson, B., Franke, A., Richter, M. and Alden, M. (1999) A Study of Homogeneous Charge Compression Ignition Combustion Process by Chemiluminescence Imaging. SAE Paper 1999-01-3680.

21 Hultqvist, A, Christensen, M., Johansson, B., Richter, M., Nygren, J., Hult, J. and Alden, M. (2002) The HCCI Combustion Process in a Single Cycle - High Speed Fuel tracer LIF and Chemiluminescence Imaging. SAE Paper 2002-01-0424.

22 Deschamps, B. and Baritaud, T. (1996) Visualization of Gasoline and Exhaust Gases Distribution in a 4-valve SI Engine; Effects of Stratification on Combustion and Pollutants. SAE Paper 961928.

23 Ghandi, J.B. and Felton, P.J. (1996) On the Fluorescent behavior of Ketones at High Temperatures. Experiments in Fluids, Vol. 21, pp. 143-144.

24 Thurber, M.C. and Hanson R.K. (1999) Pressure and Composition Dependences of Acetone Laser-induced

Fluorescence with Excitation at 248, 266, 308 nm. Applied Physics, B 69, pp. 229-240.

25 Grossman, F., Monkhause, P.B., Riddler, M., Sick, V. and Wolfrum, J. (1996) Temperature and Pressure Dependence of Laser Induced Fluorescence of Gas-Phase Acetone and 3-pentanone. Applied Physics, B 62, pp. 249-253.

26 Grossman, F., Monkhouse, P.B., Riddler, M., Thurber, M.C., Grisch, F., Kirby, B.J., Votsmeier, M. and Hanson R.K. (1998) Measurement and Modelling of Acetone Laser-Induced-Fluorescence with Implications for Temperature Imaging Diagnostics. Applied Optic, **37**, 21, pp. 4963-4978.

27 Fujikawa, T., Hattori, Y. and Akihama, K. (1997) Quantitative 2-D Fuel Distribution Measurements in an SI Engine Using Laser-Induced Fluorescence with Suitable combination of Fluorescence Tracer and excitation Wavelength. SAE Paper 972944.

28 Strand, T.E., Rothamer, D.A. and Ghandi, J.B. (2001) Flame Structure Visualization of Stratified Combustion in a DISI Engine via PLIF. SAE Paper 2001-01-3649.

29 Rothamer, D.A. and Ghandi, J.B. (2003) Determination of Flame-Front Equivalence Ratio During Stratified Combustion.SAE Paper 2003-01-0069.

30 Kashdan, J.T. and Bruneaux, G. (2004) Mixture Preparation and Combustion via LIEF and LIF of Combustion Radicals in a Direct-Injection, HCCI Diesel Engine. SAE Paper 2004-01-2945.

31 Böckle, S., Kazenwadel, J., Kunzelmann, T., Shin, D.I., Schulz, C. and Wolfrum, C. (2000) Simultaneous Single-Shot Laser-Based Imaging of Formaldehyde, OH, and Temperature in Turbulent Flames. Proceedings of the Combustion Institute, **28**, pp. 279-286.

32 Graf, N., Gronki, J., Schulz, C., Baritaud, T., Cherel, J., Duret, P. and Lavy, J. (2001) In-Cylinder Combustion Visulization in an Auto-igniting Gasoline Engine using Fuel Tracer and Formaldehyde-LIF Imaging. SAE Paper 2001-01-1924.

33 Kashdan, J.T. and Papagni, J.F. (2005) LIF Imaging of Auto-Ignition and Combustion in a Direct Injection Diesel-Fuelled HCCI Engine. To be published at Powertrain and Fluid Systems SAE Conference, San Antonio, October.

34 Bruneaux, G., Augé, M. and Lemenand, C. (2004) A study of Combustion Structure in High-Pressure Single Hole Common Rail Direct Injection Using Laser Induced Fluorescence of Radicals. Proc. COMODIA 2004, Yokohama, Japan.

35 Jeuland, N., Montagne, X. and Duret, P. (2003) Engine and Fuel-Related Issues of Gasoline CAI (Controlled Auto Ignition) Combustion. SAE Paper 2003-01-1856.

36 Pischinger, S., Lang, O., Salber, W. and Dilthey, J. (2004) Development Status of the Controlled Auto-Ignition Combustion Process. FISITA 2004 Congress, Barcelona.

37 Koopmans, L., Backlund, O. and Denbratt, I. (2002) Cycle to Cycle Variations: Their Influence on Cycle resolved Gas Temperature and Unburned Hydrocarbons from a Camless Gasoline Compression Ignition Engine. SAE Paper 2002-01-0110.

38 Dec, J.E. and Sjöberg, M. (2003) A Parametric Study of HCCI Combustion - The Sources of Emissions at Low Loads and the Effects of GDI Fuel Injection. SAE Paper 2003-01-0752.

Final manuscript received in November 2005